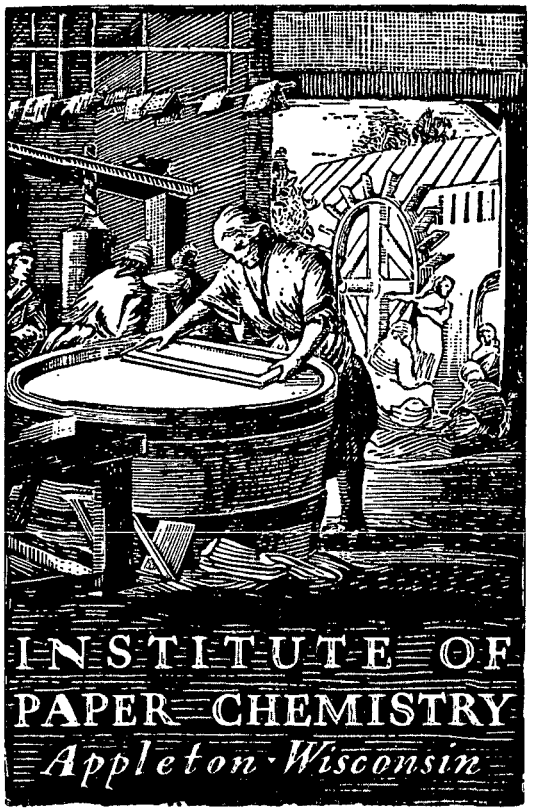

PULP TRANSPORT IN THE DISK REFINER

Project 3384

Report Two

A Progress Report

to

MEMBERS OF THE INSTITUTE OF PAPER CHEMISTRY

May 15, 1979

THE INSTITUTE OF PAPER CHEMISTRY

Appleton, Wisconsin

PULP TRANSPORT IN THE DISK REFINER

Project 3384

Report Two

A Progress Report

to

MEMBERS OF THE INSTITUTE OF PAPER CHEMISTRY

May 15, 1979

TABLE OF CONTENTS

THE INSTITUTE OF PAPER CHEMISTRY

Appleton, Wisconsin

PULP TRANSPORT IN THE DISK REFINER

SUMMARY

A disk refiner was constructed of clear Plexiglas so that high-speed motion pictures could be made of the fluid mechanics of the two-phase flow of the refining process. The theoretical potential for flows consisting of the imposed line pressure, centrifugal action of the rotor, and the stagnation pressure field that develops at the housing are set forth and verified experimentally. Theoretical and experimental modeling of the non-Newtonian flow in the rectangular tackle of the disk refiner is also presented.

The interaction between refining morphology and the transport of stock to, through, and away from the refiner is outlined. It is apparent that a substantial build-up of consistency occurs in the tackle of the refiner as a result of these interactions. The data demonstrate that the flow in the disk refiner is laminar and three-dimensional, consisting of at least primary, secondary, and tertiary flows. Several distinctly different refining actions can exist depending on dimensional and operating variables. These different refining actions greatly influence the refining process; heretofore they have not been well understood and, therefore, have not been widely utilized.

The average number of impacts is theoretically and empirically determined for one typical case for what is believed to be the most appropriate refining mode, herein termed the sweep mode of refining. Knowledge of the disk refiner transport phenomena has set the stage for refiner designs which can allow greatly reduced energy consumption. In addition, close control of refining actions for quality improvement and control will be possible.

INTRODUCTION

Little fundamental work on flows involving fiber suspensions has been accomplished other than overall pressure drop measurements largely because of the limited utility of conventional anemometry. The present effort was initiated with the objectives of ascertaining the worth of high-speed photography as an experimental means to study the fluid mechanics of such systems and to gain a preliminary understanding of the mechanics of one specific flow. The disk refiner was chosen as the flow apparatus to be filmed because the disk refiner is an important industrial process about which there is little known. Substantial conjecture has been put forth, however, by a good many authors.

It would seem that the high-speed photographic technique, properly exploited, would yield insight into the mechanism of drag reduction, flocculation, and fiber/water interaction in both laminar and turbulent flows as well as provide a means to make flow visualization and velocity measurements. There is mention in the literature of past attempts to use high-speed photography (both motion pictures and stills) to study fiber/fluid systems (1,2). It is pointed out that the films were not sufficiently clear to allow projection and viewing (1). However, some deductions were made based upon the films. Recent advances in this field (3), however, have made possible a much broader use of photographic techniques, and application to fiber/water systems seems appropriate at this time.

For analysis, it is reasonable to divide the process into subunits separating the refining morphology of the fiber from the transport of the stock to, through, and away from the refining zone. It is not clear that a complete description of the action of the disk refiner can be developed by treating refining completely separate from transport, but in this research, transport is to receive the greatest emphasis.

Refining is considered only in a speculative manner and only as it interacts with transport considerations and therefore requires the consideration of refining action.

DESCRIPTION OF THE VISUAL REFINER

An experimental refiner was constructed of clear Plexiglas. The twelve-inch rotor/stator pair was modeled after tackle used in a Sprout Waldron refiner. Although the experimental refiner is to scale, the tackle is a bit larger than that on the Sprout Waldron unit; the relative size is of commercial dimensions. The angular offset in the plane of the tackle of the lands and grooves for the stator and for the rotor is 10 degrees from the radial. There are 90 bars on the rotor and 90 bars on the stator with the angular offset of the tackle for the rotor and for the stator opposed (Fig. 1).

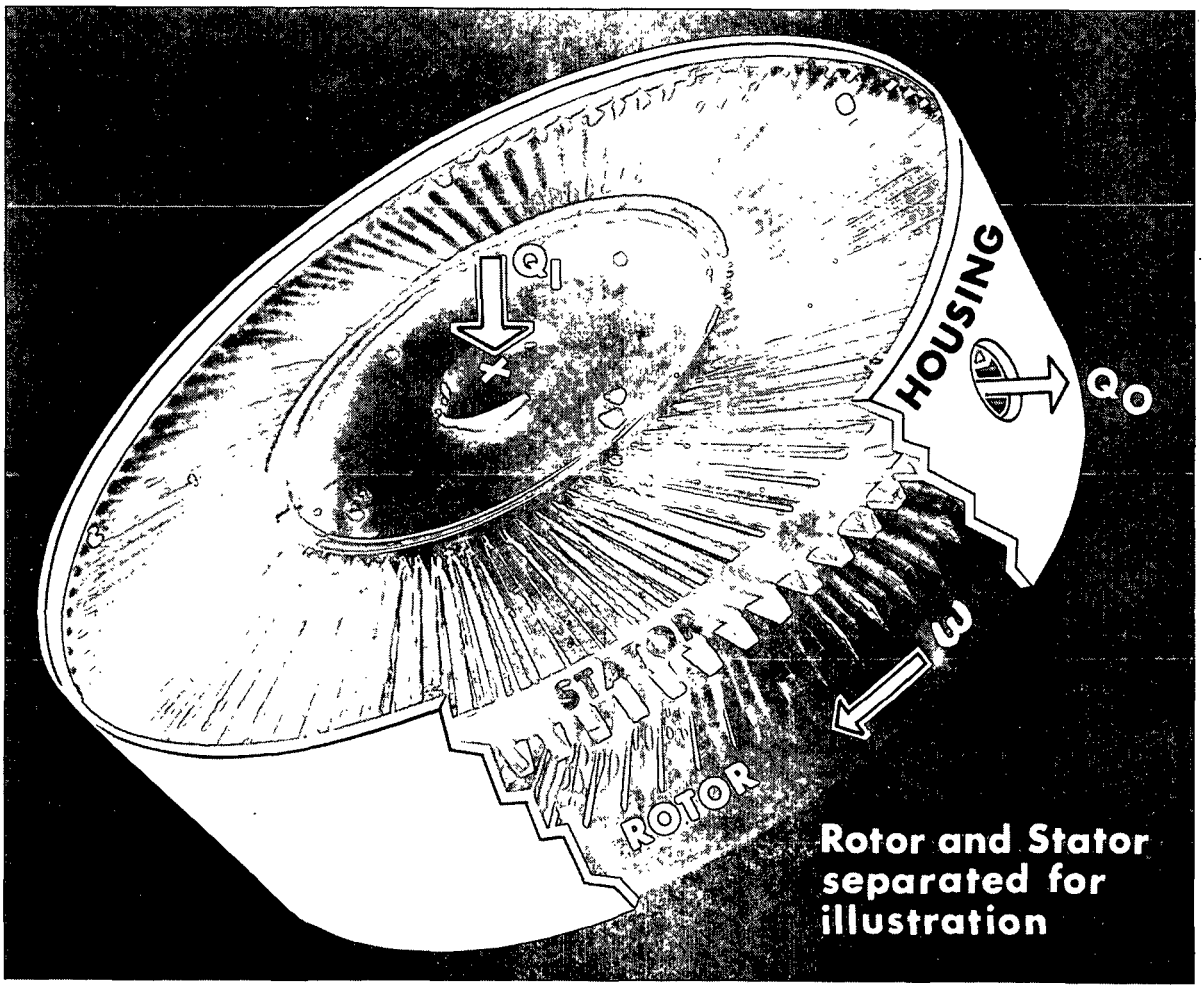

EXPERIMENTAL REFINER

Figure 1

The rotor rotates with angular velocity ω. The rotor/stator pair is enclosed in a Plexiglas housing. The flow geometry is a series of rectangular channels. There are multiple crossovers of rotor/stator bars over the radial length of the tackle as a result of the skewing of channels with respect to the radial direction (Fig. 2).

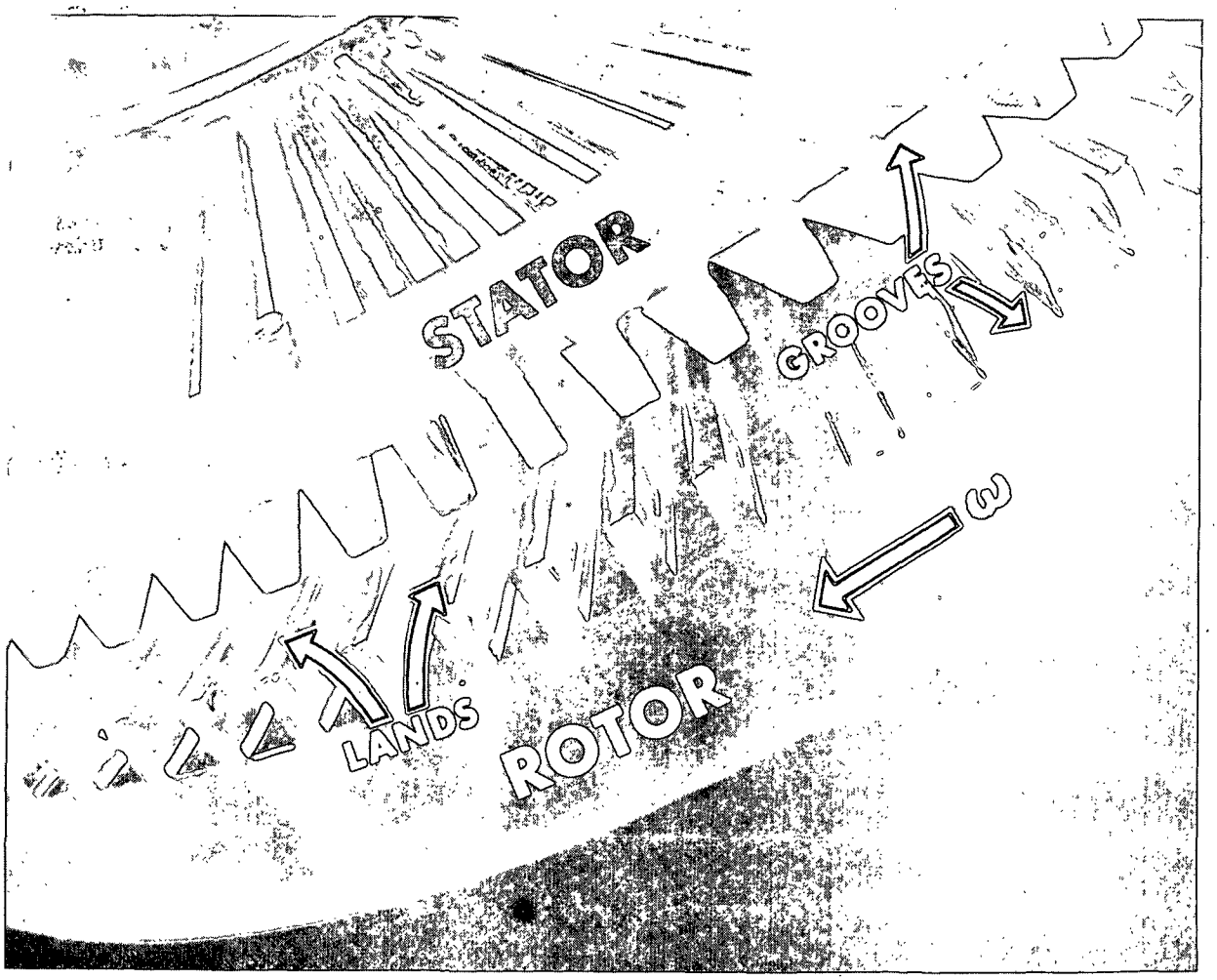

CLOSE-UP OF ROTOR/STATOR GEOMETRY

Figure 2

The first attempt that was made to film the flow of fiber in the experimental refiner was successful (Fig. 3). Note the clear definition of the tackle lands and grooves and the individual fibers stapled to the leading edge of the rotor bars. The stock contained in the tackle grooves is blurred since the camera was focused on the land of the stator.

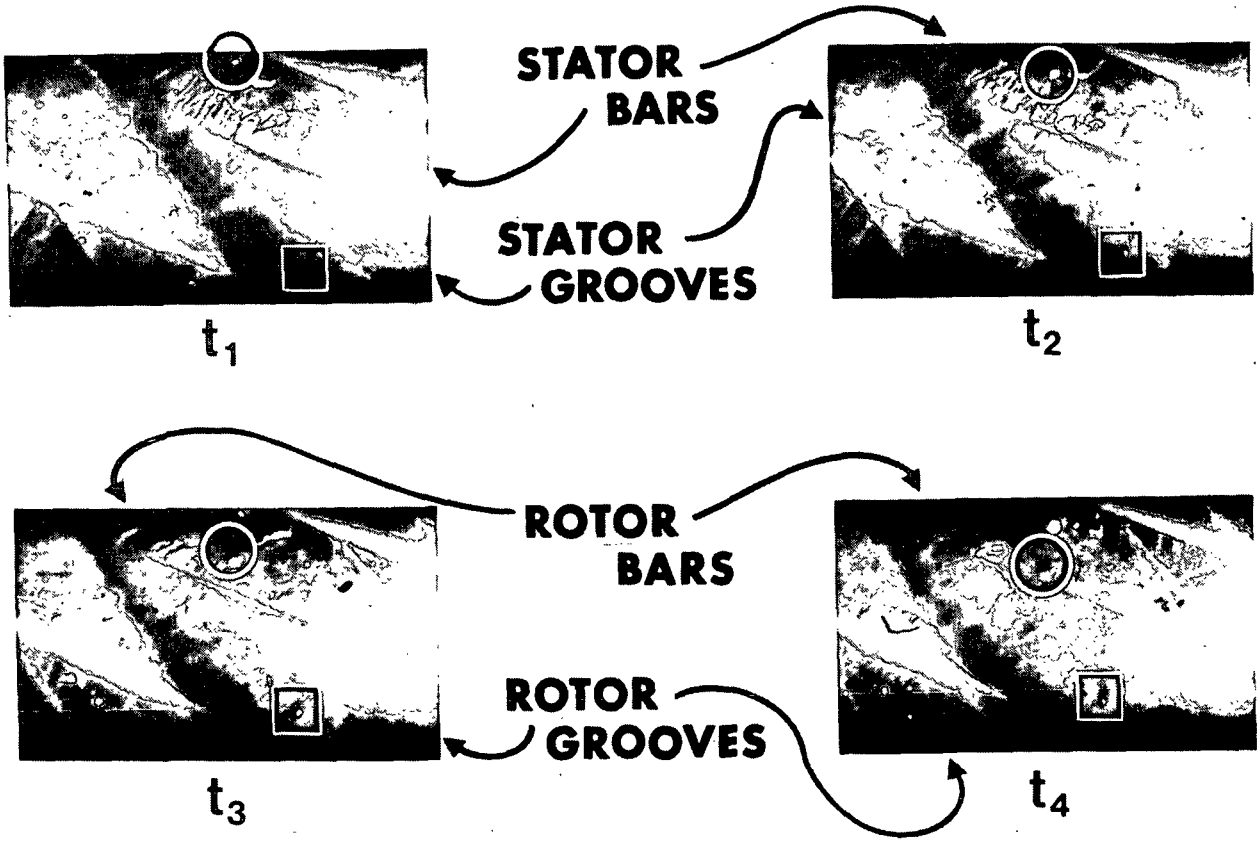

NOTES: THE CENTER OF THE REFINER IS BEYOND THE UPPER LEFT OF FRAMES.
: △ T BETWEEN FRAMES IS 1/3500 SECOND
: ① NOTE OUTWARD MOVEMENT OF AIR BUBBLE CONTAINED IN ROTOR GROOVE.
: ② NOTE INWARD MOVEMENT OF AIR BUBBLE CONTAINED IN STATOR GROOVE.
: THE VIEW IS FROM THE STATOR SIDE.

ENLARGED 16 mm FILM OF EXPERIMENTAL REFINER

Figure 3

GROSS REFINER FLOW CHARACTERISTICS

From the films, it has been observed that the flow in the refiner can be divided into two main regions, one which is arbitrarily called the circulation region and the other the exit region. The flow in, which takes place at the hub of the rotor, is designated as Q_I, and has two paths it can follow — either through the rotor (Q_I) or stator (Q_S) grooves (Fig. 4).

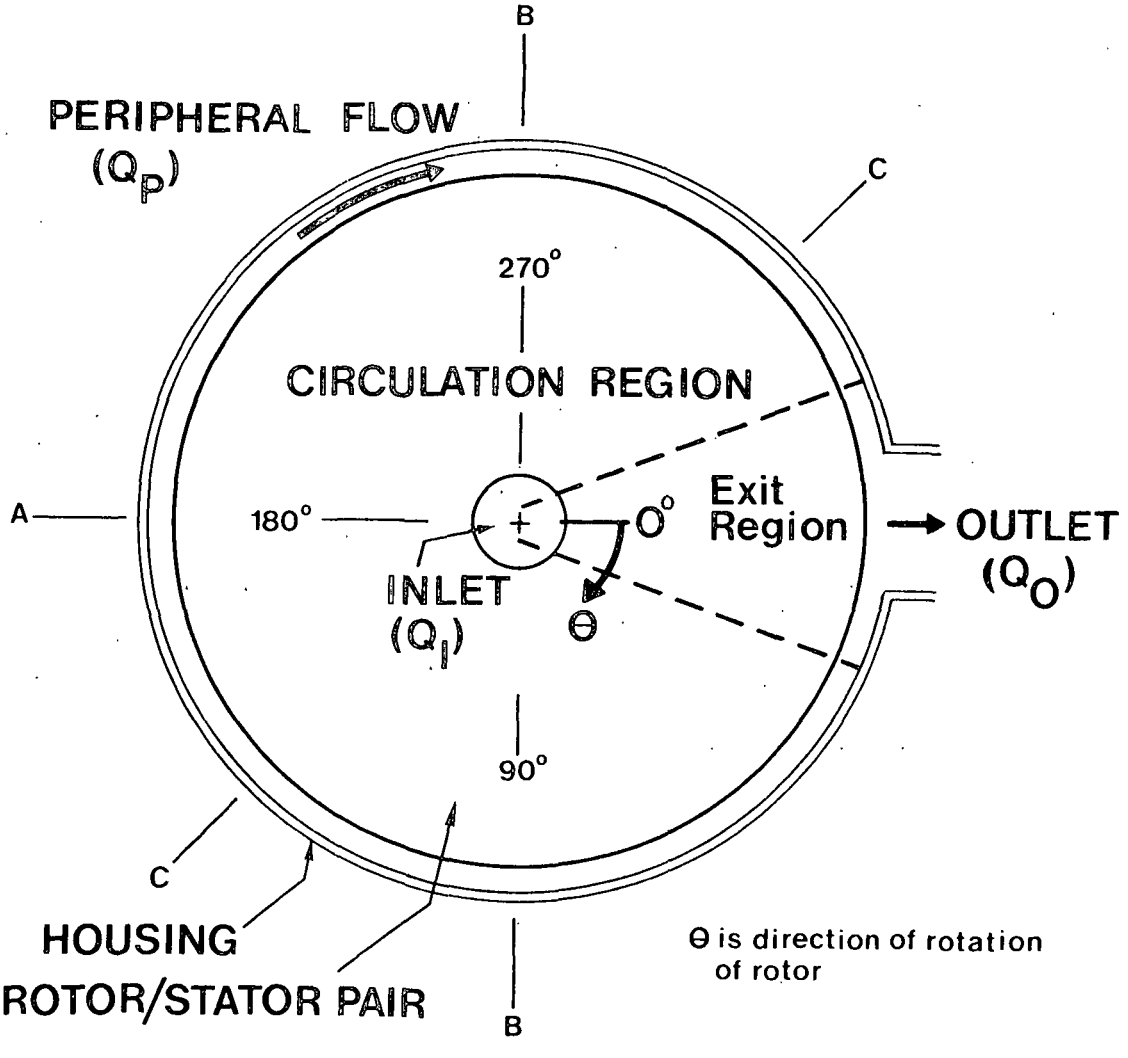

**REFINER FLOW PATTERN
SHOWING TWO MAIN REGIONS OF FLOW**

Figure 4

The direction of the flow is radially inward in the stator except in the exit region. Inward flow in the stator was not predicted in advance of experimentation, but, in fact, a very strong radial flow inward in the stator has been observed in the films. Reverse flow in the stator was, however, reported by Banks (1). This is the situation observed for what has been called the circulation region. Due to the rotational motion of the rotor, an amount of fluid will travel around the periphery of the rotor and stator (Q_P), some of which is ultimately delivered to the discharge flow from the refiner. The remainder is mixed with stock in the exit region and recirculated. It was observed that the flow in the rotor and stator are at least one order of magnitude greater than Q_I or Q_P. This requires that within the refiner there be a large recycle stream (Fig. 5). Clearly a tremendous acceleration exists in the flow loop out of the rotor and in the stator.

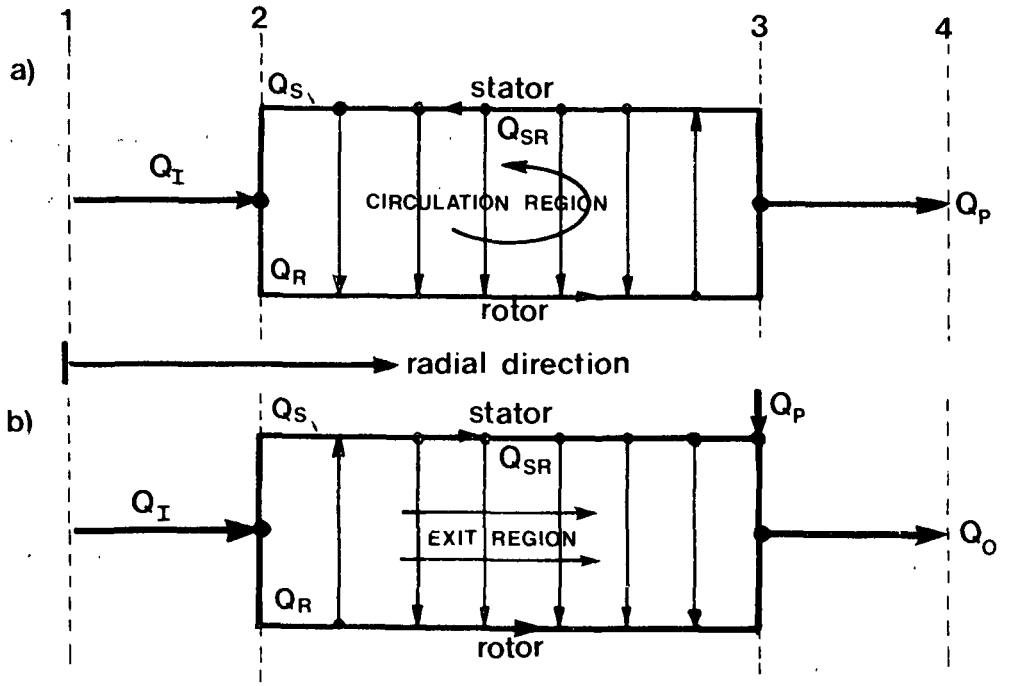

Figure 5. Overall Refiner Flow Model

In this region

$$Q_I + Q_S = Q_R \quad \text{and} \quad Q_R + Q_{SR} = Q_S + Q_{SR} + Q_P \tag{1}$$

From Equation (1), $\underline{Q}_I = \underline{Q}_P$, but $\underline{Q}_S$ does not equal $\underline{Q}_R$, unless $\underline{Q}_I$ and $\underline{Q}_P$ are zero. Also note that $\underline{Q}_R > \underline{Q}_S$.

In the exit region (Fig. 4), recirculation (inward flow in the stator) does not exist, and the flow is pictured as in Fig. 5. Here

$$Q_I = Q_R + Q_S \quad \text{and} \quad Q_O = Q_R + Q_{SR} + Q_S - Q_{SR} + Q_P = Q_R + Q_S + Q_P \tag{2}$$

where $\underline{Q}_O$ is the outlet flow and has an additional small contribution from $\underline{Q}_P$. The outward flow ($\underline{Q}_R$) in the rotor grooves, the observed inward flow ($\underline{Q}_S$) in the stator grooves, and the peripheral flow ($\underline{Q}_P$) of the fluid induced by the rotor rotation are arbitrarily called primary flows. There are a number of important induced flows that will be treated in detail in a later section.

MODEL OF PRIMARY FLOWS

As an aid in analysis, the flow is modeled as through a matched pair of rotor and stator grooves, thus providing considerable simplification (Fig. 6). The tackle of the rotor and the stator (directly opposed) is shown with no offset from the radial; thus, there are no crossovers along the radial length of the tackle. The small spacing between the rotor and the stator is ignored since in a commercial operation this gap might vary from nearly zero clearance at low angular velocity to perhaps 10 or 20 thousandths of an inch at high angular velocity. The grooves in the rotor and stator tackle might be 3/8 inch in a commercial refiner; and thus, ignoring the space between the rotor and stator is justified. In this model, that the tackle of the rotor and stator cross one another is not overlooked; as a result of the crossovers, a time-dependent boundary separates the rotor/stator loop. The boundary, intermittant as it is, has been observed to effectively separate the primary flows in the rotor and in the stator. The flow then is characterized as flow in a rectangular duct of length $\underline{\ell}$. The pressure $\Delta P_{\underline{\ell}}$, is the driving force that is forcing the fluid through the duct.

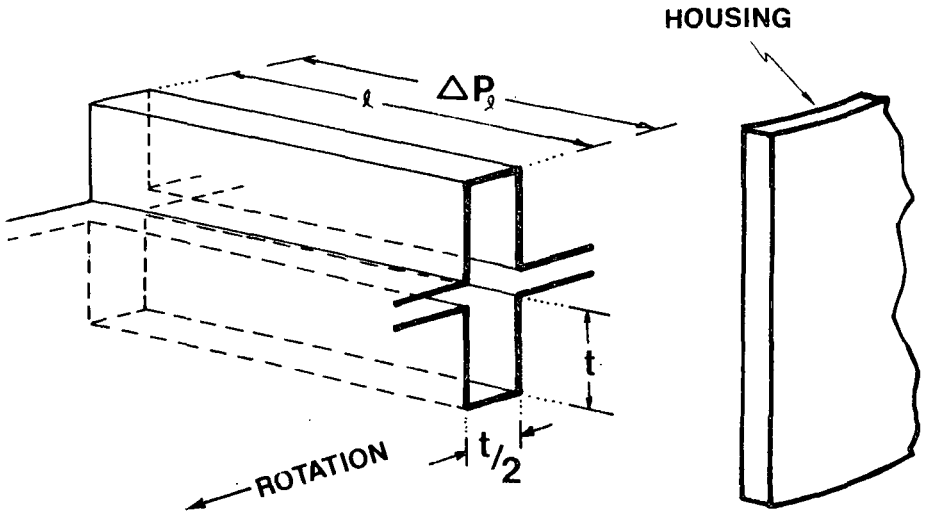

Figure 6. Model Rotor/Stator Groove Pair
(Note: The Experimental Unit has $\underline{t}$ = 0.125 inch and $\underline{\ell}$ = 3 inches)

In addition to the line pressure ΔP_{ℓ}, imposed on the refiner, another force is also operating on the fluid because of the angular velocity of the rotor. Within the groove of the rotor is a body force resultant from the centrifugal action of the rotor. This gives rise to an accelerated flow of fluid out of the grooves of the rotor. This flow decelerates and ultimately stagnates against the housing in the recirculation region and gives rise to an adverse pressure gradient that is felt by both the rotor and stator. Because the stator does not experience this body force, this adverse pressure gradient causes an inward flow in the stator grooves. Thus, a very strong flow out of the tackle of the rotor and into the tackle of the stator is created as a result of the body force acting on the fluid in the rotor grooves and is the source of the pressure necessary to drive the recirculation in the stator observed in the films.

An understanding of the total pressure field (i.e., the line pressure plus the pressure developed as a result of the stagnation of flow against the refiner housing) is attained by qualitatively estimating the line pressure, the body force, and the stagnation pressure. The approximations are empirically verified, and experimental data are presented.

THE LINE PRESSURE FIELD

Consider the full radial plane of the refiner with the flow in at the center and out of the refiner at one line along the edge (selected for the calculation to be on the right). The line pressure is the pressure that is imposed on the refiner by the upstream pump forcing the flow through the refiner. The simple model is one of potential flow, consisting of a point source and a point sink. The rotor/stator tackle separates the hub from the periphery. If the inflow is divided into decants, then lines of constant flow and lines of constant potential for flow can be established by using the Cauchy-Riemann relationship.

In polar coordinates these are

$$\frac{\partial u}{\partial r} = \frac{1}{r}\frac{\partial v}{\partial \theta} \quad ; \quad \frac{\partial v}{\partial r} = -\frac{1}{r}\frac{\partial u}{\partial \theta} \tag{3}$$

The constant potential lines are isobars or lines of constant pressure. In the absence of angular rotation of the tackle the general shapes of the flow and pressure fields are deduced (Fig. 7).

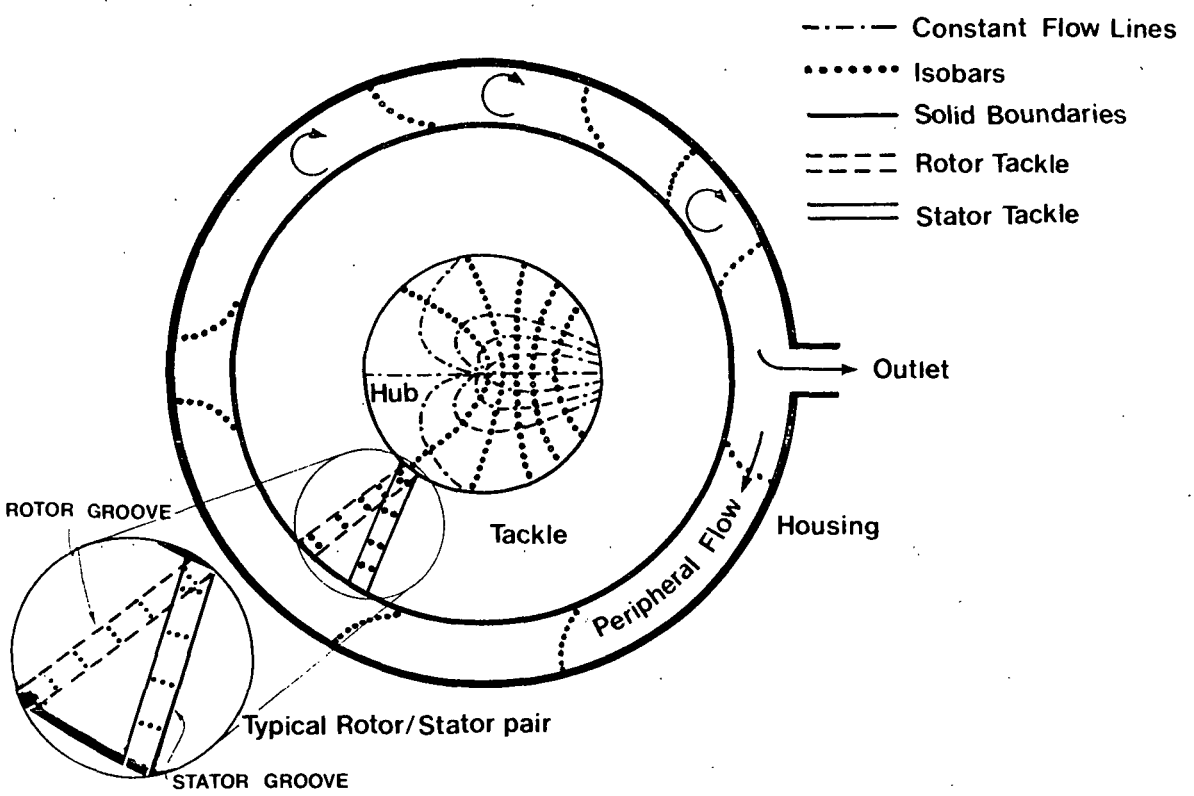

Figure 7. Pressure Field Imposed Upon Disk Refiner

The line pressure field is straight forward in the hub region of the refiner. However, at the inside boundary of the tackle, the flow configuration is substantially altered by virtue of the stator and rotor grooves. The lines of constant flow must necessarily be parallel to the tackle grooves and since rotor and stator tackle physically diverge, there will exist pressure discontinuities at the outer periphery of the tackle. These discontinuities will

result in the development of vortices (three-dimensional flow) which prevent accurate modeling using the Cauchy-Riemann equations in the periphery region of the refiner.

If the isobars are viewed in a three-dimensional model and if the flow lines are omitted, the pressure field (and pressure gradients) are somewhat easier to visualize (Fig. 8). Thus, the incoming flow experiences a high pressure, and the outflow experiences a minimum pressure with respect to line pressure. There is little pressure gradient in the region A as a result of the line pressure, but on a line between the inlet and the exit, there is a strong pressure gradient imposed that will add to the centrifugal body force that exists to force flow outward in the rotor.

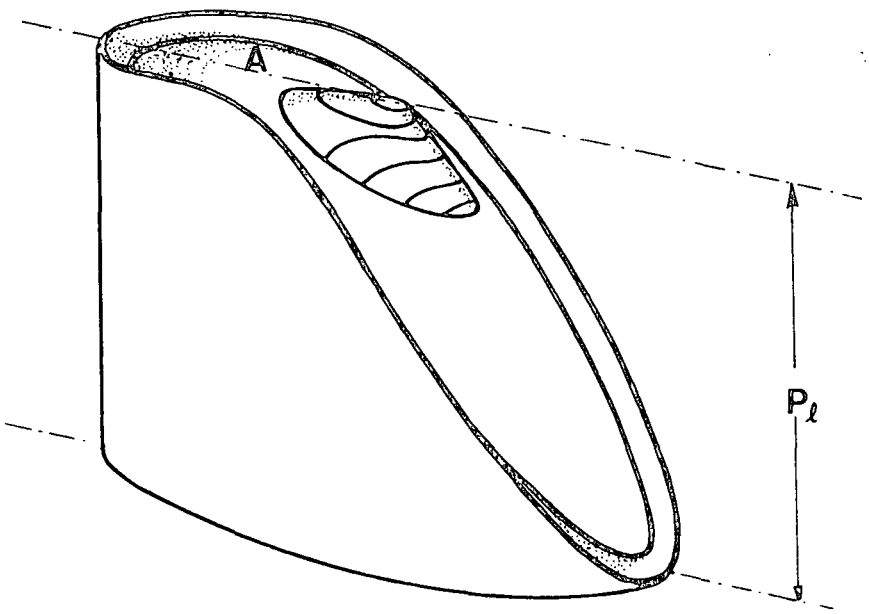

Figure 8. Three-dimensional Imposed Pressure (Hub, Stator, and Periphery)

The pressure field in the plane of the rotor is expected to be nearly identical to that of the plane of the stator except that through the tackle, the angular sense of the direction of flow is rotated 20 degrees clockwise with

respect to the flow through the stator. The estimate of the pressure field existing in the periphery where there is mixing due to the three-dimensional flow caused by the pressure discontinuity is qualitatively estimated regardless of the three-dimensionality of flow that prevails.

The lines of constant potential for flow (pressure) are established by a conformal mapping technique. The flow in the refiner z-space in the absence of the tackle is mapped by the transformation

$$\zeta = i\left(\frac{r_o - z}{r_o + z}\right) \tag{4}$$

where $\underline{r}_o$ is the radius of the refiner onto the upper half-plane in the ζ-space. This takes the source from $\underline{z} = 0$ to $\zeta = \underline{i}$ and the sink from $\underline{z} = \underline{r}_o$ to $\zeta = 0$. The periphery of the refiner appears as the real axis in the ζ-space. By locating two sources, each of strength $\underline{m}$, in the ζ-space at $\zeta = \underline{i}$ and $\zeta = -\underline{i}$ and a sink of strength $2\underline{m}$ at $\zeta = 0$, we can calculate the complex potential Ω for the flow, which is found to be

$$\Omega = -m \log\left(\frac{\zeta^2 + 1}{\zeta^2}\right) \tag{5}$$

In the z-plane, the complex potential is:

$$\Omega = -m \log\left(\frac{(r_o - z)^2 - (r_o + z)^2}{(r_o - z)^2}\right) \tag{6}$$

(see Fig. 9).

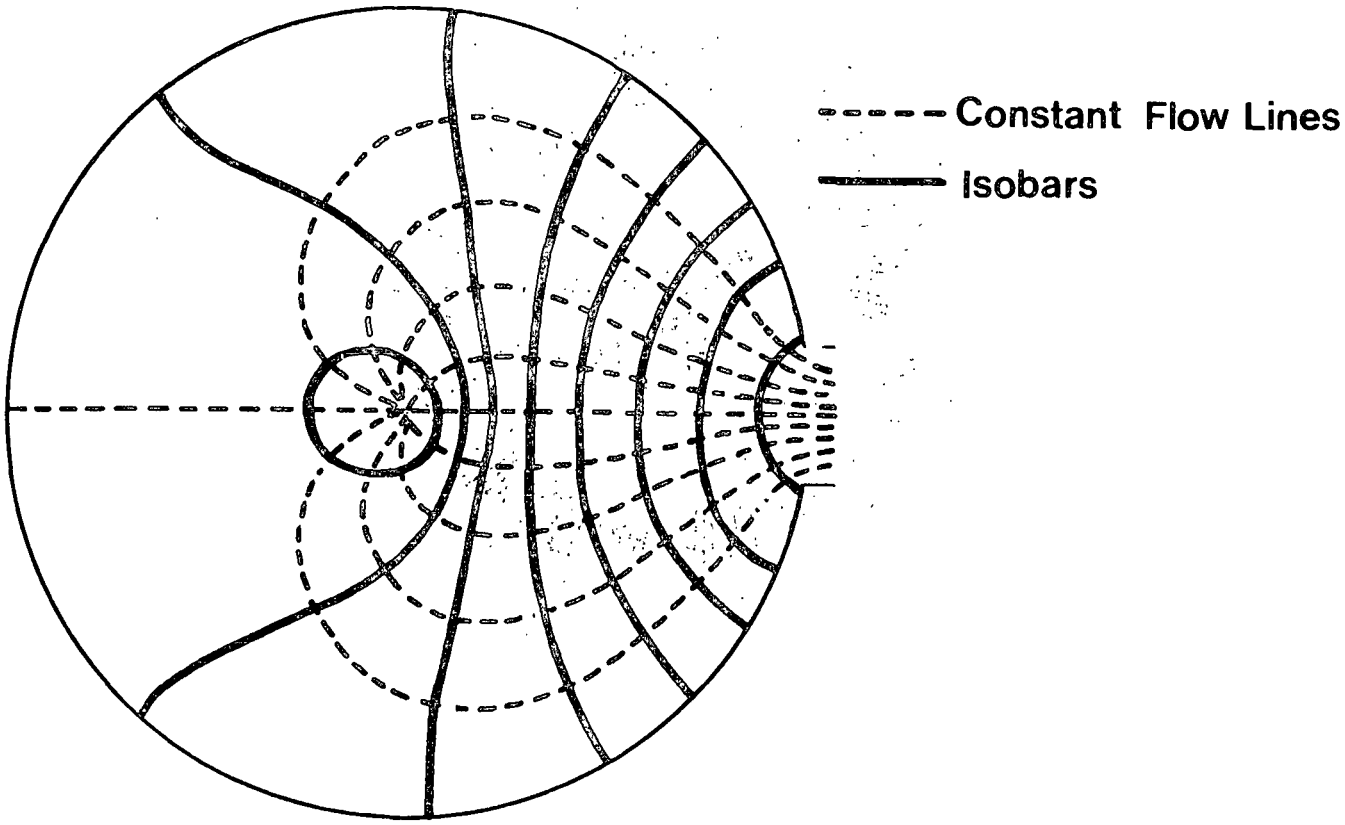

Figure 9. Pressure Field Imposed on Disk Refiner Neglecting the Presence of the Tackle

This may be expressed in rectangular coordinates as

$$\Omega = m \log \left[\frac{4r_o \sqrt{x^2 + y^2}}{(x - r_o)^2 + y^2} \right] + i \left[\tan^{-1}\left(\frac{y}{x}\right) - 2\tan^{-1}\left(\frac{y}{x - a}\right) \right] \qquad (7)$$

The equipotential lines are then given by the real part of the complex potential

$$\text{Re } [\Omega] = \Phi = m \log \left[\frac{4r_o \sqrt{x^2 + y^2}}{(x - r_o)^2 + y^2} \right] = \text{constant} \qquad (8)$$

The experimentally determined pressure field resulting from line pressure alone is seen to compare qualitatively in a favorable way to that which was predicted by physical reasoning alone (Fig. 10).

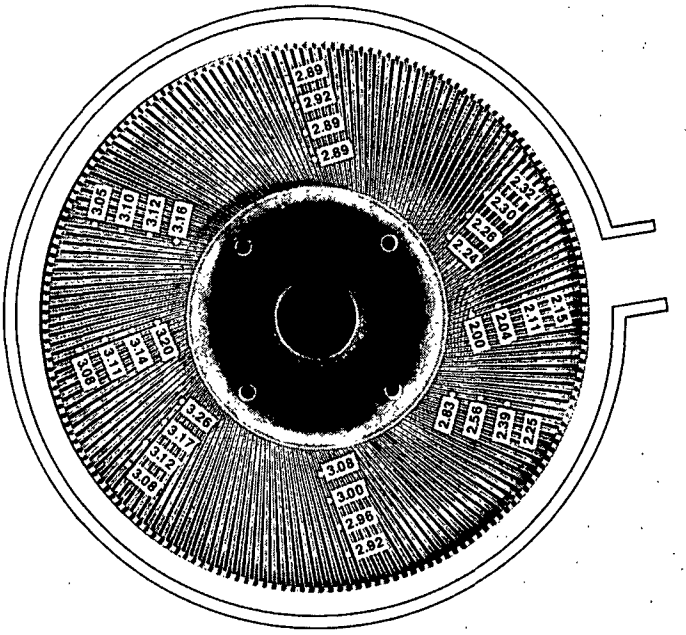

Figure 10. Imposed Stator Line Pressure (Note: 1. Pressures Are in Feet of Water. 2. Flow Rate is 8 Cubic Feet per Minute)

THE BODY FORCE

The body force due to the centrifugal action in the rotor that a unit volume of fluid will experience is zero at the center of the plane of the refiner and is maximum at the periphery of the rotor (Fig. 11). This force coupled with the line pressure gives rise to the motion of the fluid in the refiner rotor. Indeed, if line pressure were zero and the refiner were full of stock of any consistency and the rotor rotated with any angular velocity, there would be a flow outward in the grooves of the rotor. This flow stagnates against the housing, creating an adverse pressure gradient which forces the fluid back in the stator toward the hub.

The measured adverse pressure gradient resulting from stagnation of radial flow against the housing is presented in Fig. 12.

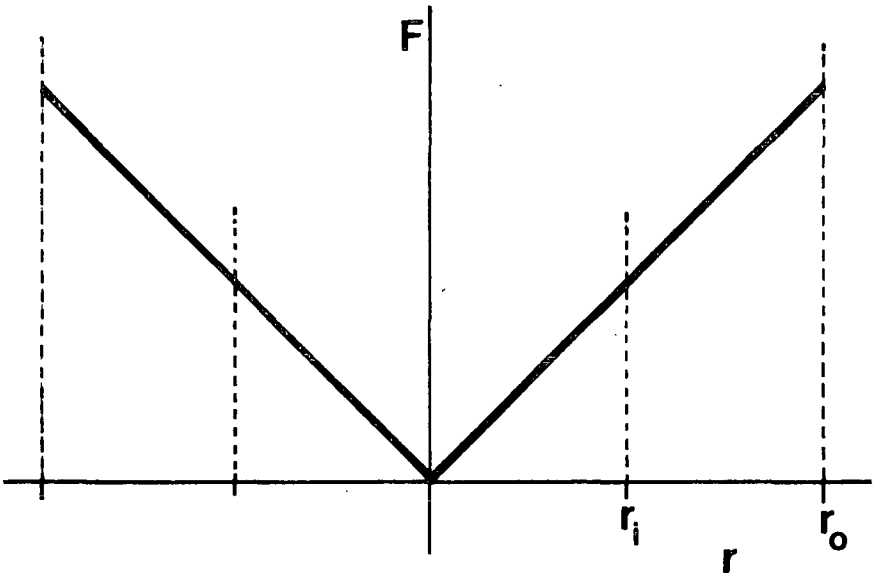

Figure 11. Imposed Body Force on the Rotor

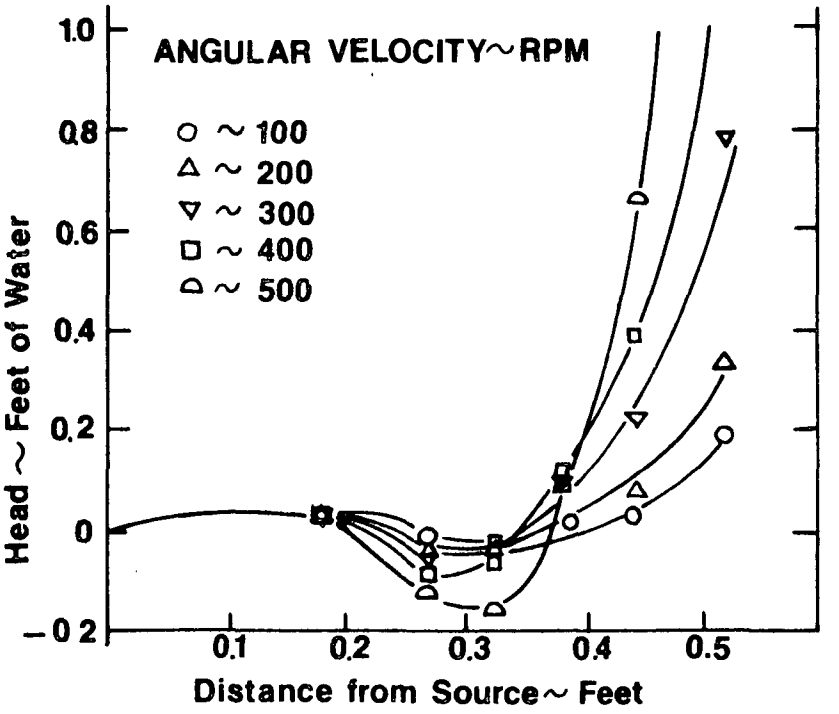

Figure 12. Stagnation Pressure on the Refiner

Pressure losses due to friction should also be taken into account. These are estimated through the use of the standard Fanning friction factor versus Reynolds number curve for Newtonian fluids. As will be shown later, the flows of commercial interest are strictly laminar. Schlichting gives expressions for the friction factor f for laminar flow in rectangular ducts of various aspect ratios (ratio of height to width). For an aspect ratio of 1:1, he gives $4f = 57/Re$ and for 3.5:1, $4f = 71/Re$ (4). This work has involved rectangular channels with aspect ratios of 2:1. Thus as a first approximation, we will use the relation derived for laminar flow in a circular pipe; namely, $4f = 64/Re$.

THE TOTAL PRESSURE FIELD

Two potentials for flow have been mapped out for pulp transport in the refiner. One is the imposed line pressure across the refiner and the second is the body force that gives rise to an adverse pressure gradient. Considering again the plane of the tackle, it is not difficult to recognize that the pressure field experienced by the fluid depends on where on this plane the fluid is located at any given time (Fig. 4). Consider for descriptive clarity three cases: Plane AA, BB, and CC. Case one, the Plane AA, is through the center of the refiner (the source) and the outflow (the line sink); Plane BB is at right angles to the plane of case one, and Plane CC is at 45 degrees to either. Through the Plane AA upstream on a line drawn through the inflow and the outflow of the refiner, there exists a flat plateau of little pressure gradient and about of equal pressure to the line pressure (Fig. 13). In the region downstream on the line from the inflow to the outflow, there is roughly a linear relationship between the pressure and position within the refiner. Adding to this line pressure field, the pressure that results from the stagnation of the flow induced by the body force, some physical understanding can be gained of the flow field. Upstream of the inflow,

a dynamic contribution is made as upstream flow stagnates against the housing, but downstream in the exit region, there is no contribution because there is no housing wall against which the flow may stagnate; therefore, no adverse pressure gradient exists downstream. If we assume that the two sources of flow potential may be added (a linear problem), we get the third sketch of Fig. 13a, b, and c. Clearly, recirculation will occur upstream but would not be expected downstream.

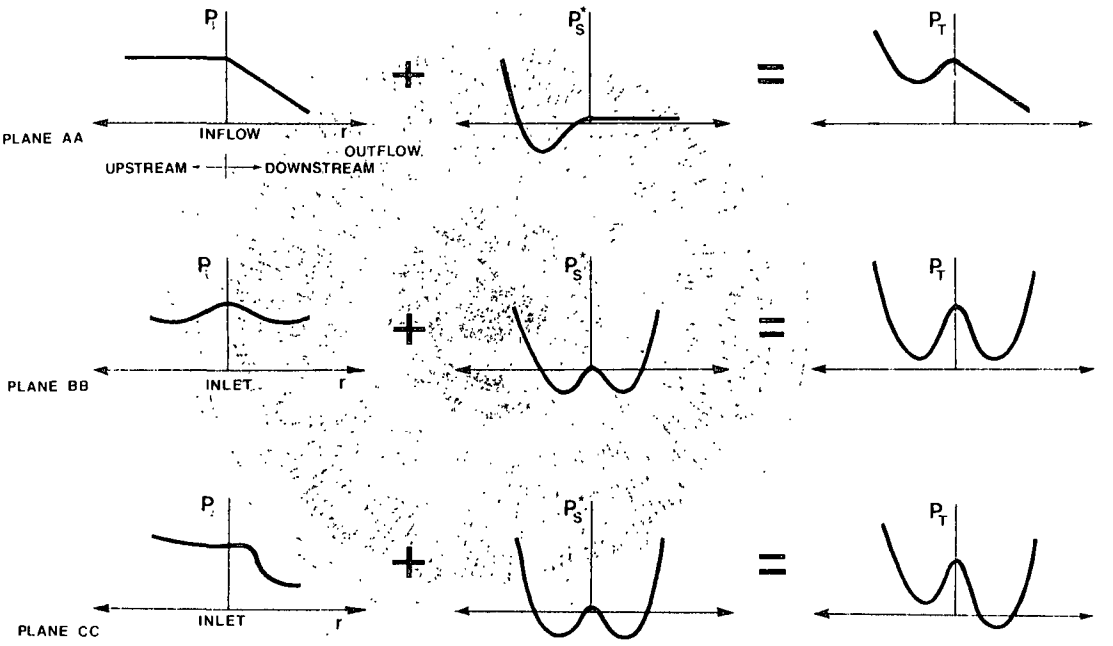

Figure 13. Qualitative Estimate of Refiner Total Pressure Field
a) Along Plane AA, b) Plane BB, c) Plane CC
(Note: P_S^* = Stagnation Pressure)

A different situation exists for cross section BB. The line pressure is a peak at the inlet, decreases radially outward, and then increases slightly toward the outer radius of the refiner. Since there is a housing on each side, an adverse pressure gradient is established, and recirculation should occur. For the third pressure profile to be mapped (Plane CC), the line pressure is higher on the upstream side of the source than the downstream side because the fluid is near the plateau, but it does not go to zero because of the wall on this side.

The stagnation pressure is symmetrical, as before, since stagnation exists on both sides due to the presence of the housing.

The total static pressure field was measured with a water manometer (Fig. 14). Note that the acceleration of the stock can cause a substantial decrease in pressure. Thus, if ω is high enough, for any given Q_{in}, cavitation may result.

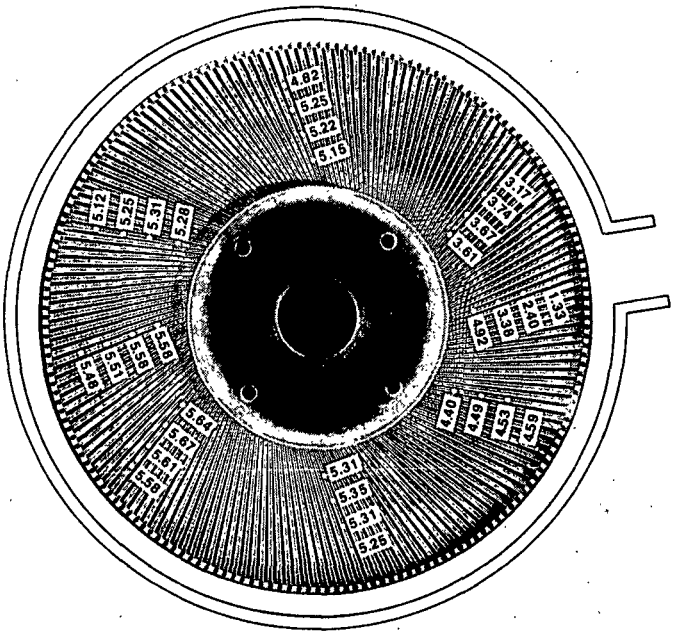

Figure 14. Total Pressure on the Refiner (Note: 1. Pressures Are in Feet of Water. 2. Flow Rate is 0.134 Cubic Feet per Second. 3. Angular Velocity is 400 Revolutions per Minute)

As seen from the previous analysis, the only place where a reverse flow in the stator is not expected is in the region close to a line between the inflow and the outflow that has been called the exit region (see Fig. 4). This expectation derives from the flow not stagnating on this plane and thus, there exists no potential to give rise to a reverse flow. The reverse flow, therefore, exists from the leading edge of the outflow around the refiner to the trailing edge of the outflow. Along the line from the inflow to the outflow, the outflow in the stator is caused

largely by the line pressure plus the effect of being dragged along by the outward flow in the rotor where it is intermittently in contact with the rotor at the interface. The flow in the rotor along this same line is caused by line pressure plus the body force. The body force is proportional to the radius of the rotor and the angular velocity of rotation squared.

FLOW IN THE GROOVES

The easiest way to analytically approximate flow in a rectangular duct such as this is to use an equivalent circular geometry and a hydraulic radius concept. Approximation as a channel may not be as accurate because of the low aspect ratio and the fluid surface between the rotor and stator grooves. Furthermore, in the recirculation region, the rotor and stator grooves should be modeled separately, while in the exit region they could be modeled together.

For one groove

$$r_H = \frac{\text{cross-sectional area}}{\text{wetted perimeter}} = t/5 \tag{9}$$

which is exactly the same if a rotor/stator pair is considered (Fig. 5). The equivalent radius and diameter are given by

$$2r_e = d_e = 4r_H = 4t/5 \tag{10}$$

and pipe flow equations can be used with d replaced by d_e. The stress for the flow is

$$\tau = -\frac{r_e}{2}\frac{dp}{dL} \tag{11}$$

and the average velocity would be given by

$$\bar{v} = -\frac{r_e^2}{8\mu}\frac{\Delta p}{\ell} \tag{12}$$

if the flow can be assumed laminar and if there are no entry effects.

The flow rate can be obtained by further integration to give

$$Q = - \frac{\pi r_e^4}{8\mu} \frac{\Delta p}{\ell} \tag{13}$$

Fiber/water suspensions are actually quite non-Newtonian and this is not taken into account in this model. Also, recall that entry effects have been neglected. A more accurate analysis (but still more simplified than the real situation) is given as follows:

If it is assumed that the flow is laminar and fully developed with no entry length effects, the velocity distribution $\underline{u}(\underline{y},\underline{z})$ in the stator and rotor may be obtained. If there are no secondary flows, the equations of motion in rectangular coordinates reduce to:

$$\text{Continuity:} \qquad \frac{\partial u}{\partial x} = 0$$

$$\text{X-Momentum:} \qquad 0 = - \frac{\partial p}{\partial x} + \mu \left(\frac{\partial^2 u}{\partial y^2} \frac{\partial^2 u}{\partial z^2} \right) \tag{14}$$

$$\text{Y-Momentum:} \qquad 0 = - \frac{\partial p}{\partial y}$$

$$\text{Z-Momentum:} \qquad 0 = - \frac{\partial p}{\partial z}$$

subject to the no-slip condition on the walls. The total pressure gradient $\partial \underline{p}/\partial \underline{x}$ is a combination of several factors: the imposed line pressure, the stagnation pressure, and the pressure losses due to drag. There is also the body force influencing flow in the rotor, and this must be incorporated into the equations of motion in a more thorough analysis that would be intended to predict flow in the rotor.

Since $\underline{p} = \underline{p}(\underline{x})$ only, we must have that

$$\frac{\partial^2 u}{\partial y^2} + \frac{\partial^2 u}{\partial z^2} = \frac{1}{\mu} \frac{dp}{dx} = \text{constant} \tag{15}$$

An exact solution to the above equation is known for steady flow through a rectangular section of height 2a and width 2b. The average velocity $\bar{u}$ is given by (6).

$$\bar{u} = \frac{a^2}{3\mu} - \frac{dp}{dx}\left[1 - \frac{192a}{\pi^5 b}\sum_{i=1,3,5\ldots}^{\alpha}\frac{\tan h\,\frac{i\pi b}{2a}}{i^5}\right] \qquad (16)$$

for the stator.

VISCOSITY

There are many questions about the viscous behavior of fiber/water systems. In the absence of a complete treatise on the subject, it is assumed that the apparent viscosity as reported by Guthrie (8) is adequate to allow some deduction about the flow in the subject refiner (Fig. 15).

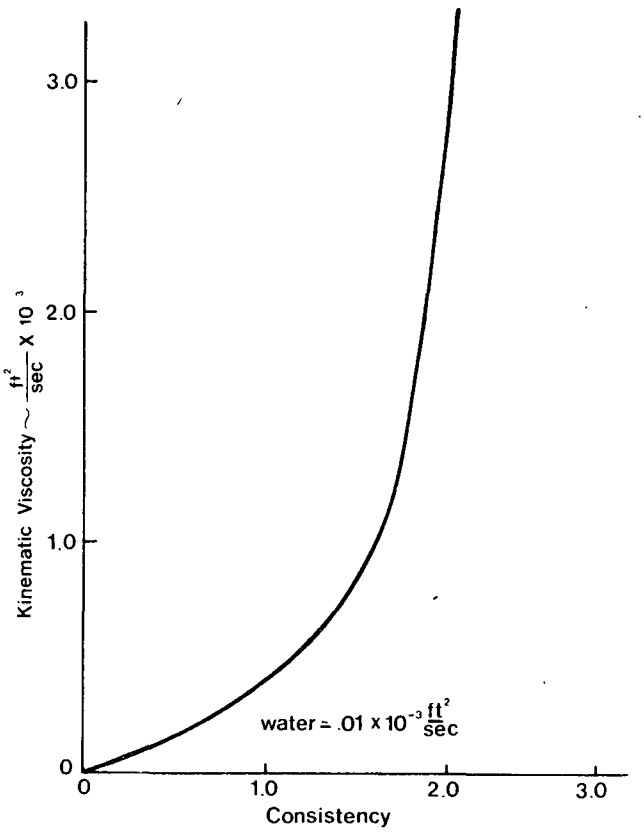

Figure 15. Viscosity of Pulp Suspensions

AN ORDER OF MAGNITUDE ANALYSIS

To determine the Reynolds number, we measure the average velocity through the tackle from the geometry and the overall flow rate. The total cross-sectional area for both the rotor and stator is

$$A = t^2 N \tag{17}$$

where N is the number of grooves. With t = 3/8 inch and N = 90

$$A = 0.09 \text{ ft}^2 \tag{18}$$

For flow of 25 gal/min, which is about 0.05 ft^3/sec, the velocity is expected to be

$$U_I = 0.56 \text{ ft/sec} \tag{19}$$

However, this does not take into account the large recirculation flow as caused by the body force. The equivalent diameter from Equation (10) gives

$$d_e = 4t/5 = 0.025 \text{ ft} \tag{20}$$

A Reynolds number using the overall average velocity from Equation (19) is

$$N_{Re} = \frac{U_I d_e}{\nu} = 1400 \tag{21}$$

if the material were water. For a 2% slurry, the Reynolds number would be reduced to less than 5. If all the flow went through either the rotor or the stator, the area for flow would be reduced by one half, and the velocity U_I, would be doubled. Since d_e does not change, the values for the Reynolds number would be doubled. Although these Reynolds numbers are low enough to justify the assumption of laminar flow, if U_I were the correct velocity, recirculation does occur and must be estimated.

Measurements have been made from the films of 5-10 ft/sec inward in the stator at an input consistency of 0.1% and a rotation rate of 200 rpm. For a 0.1% consistency slurry, this would give

$$N_{Re} = \frac{\bar{u} d_e}{\nu} = \frac{5(0.025)}{0.04 \times 10^{-3}} = 3100 \qquad (22)$$

using ν from Fig. 15. For a 2% consistency material, the Reynolds number is less than 30. Thus the flow is in all probability laminar for any practical cases. Furthermore, note that the experimentally measured velocity of 5 ft/sec is much greater than $\underline{U_I}$ estimated at 0.56 ft/sec; thus, we see that the flow recirculation as a result of the body force predominates.

CALCULATED VELOCITY AND PRESSURE DROP

Velocity measurements were made at an input consistency of 0.1% and at 200 rpm. The measured velocity in the stator was $\underline{\bar{u}_m} = 5.0$ ft/sec.

Since we have assumed a laminar flow situation, then

$$\bar{u} = \frac{a^2}{3\mu} - \frac{\Delta p}{l}\left[1 - \frac{192a}{\pi^5 b} \sum_{i=1,3,5\ldots}^{\alpha} \frac{\tanh \frac{i\pi b}{2a}}{i^5}\right] \qquad (23)$$

where

$$-\Delta p = P_L + P_d + P_{drag}$$

$$= 1 + 1/2\ \rho\omega^2\ (r_o^2 - r_i^2) + \frac{2f\rho \bar{u}_m^2 \Delta l}{d_e} \qquad (24)$$

$$= 255\ lb_f/ft^2$$

Assuming μ to be that of water,

$$\bar{u} = 735\ \text{ft/sec} \qquad (25)$$

This is two orders of magnitude greater than was experimentally observed; thus we must have a much higher μ than for water. By a trial-and-error procedure, various values of μ are chosen until $\bar{u} = \underline{\bar{u}}_m$. This occurs for $\mu = 8.7 \times 10^{-2}$ $lb_m/ft\text{-}sec$ or $\nu = \mu/\rho = 1.4 \times 10^{-4}$ ft^2/sec which corresponds to a consistency in the stator of approximately 1.75%. Since the input consistency is known to be 0.1%, the consistency in the refiner tackle must be greatly amplified by the mechanics of the pulp transport.

An alternate analysis can be performed which leads us to the same result. Using the modified pipe flow Equations (12) and (13), and if we let μ be that for water, we have

$$\bar{u} = \frac{-r_e^2}{8\mu} \frac{\Delta p}{\ell} = 1000 \text{ ft/sec} \tag{26}$$

Using our experimental data

$$\mu = \frac{-r_e^2 \Delta p}{8\bar{v}\ell} = 0.128 \text{ } lb_m/ft\,sec \tag{27}$$

$$\nu = \frac{\mu}{\rho} = 2.05 \times 10^{-3} - ft^2/sec$$

which corresponds to a consistency of approximately 1.9%.

We are, therefore, led to conclude that flow in the refiner is laminar for all cases where the feed consistency is 0.1 or greater.

ENTRY LENGTH

Equations (12) and (23) can be used with minimal error in calculations if there is no entry loss effect. The importance of an entry loss can be determined for laminar flow (10). For a 2% consistency stock and for flow through only 10% of the tackle length

$$100 \frac{x/d_e}{Re} = 2.5 \tag{28}$$

From Fig. 16 we can see that for a value of 2.5, the flow has obtained approximately 80% of its fully developed value. Thus, we may neglect entry length effects for this analysis. An independent check can also be performed (Fig. 17). The term

$$N_E = \frac{x/d_e}{N_{Re}} = \frac{1}{4}\frac{x\nu}{r_e^2\,\bar{u}} \tag{29}$$

is the parameter of importance. For the 0.1% case

$$\frac{x/d_e}{N_{Re}} = \frac{0.25/0.025}{310} = 0.032 \tag{30}$$

where x is taken as ℓ = 3 inches, one half the refiner radius.

For a 2% consistency, the parameter becomes 0.25. From the work of Langhaar (5) (Fig. 16), the excess entry pressure drop is usually considered negligible if the parameter is greater than 0.1. Therefore, the entry length is negligible in any flow of commercial interest.

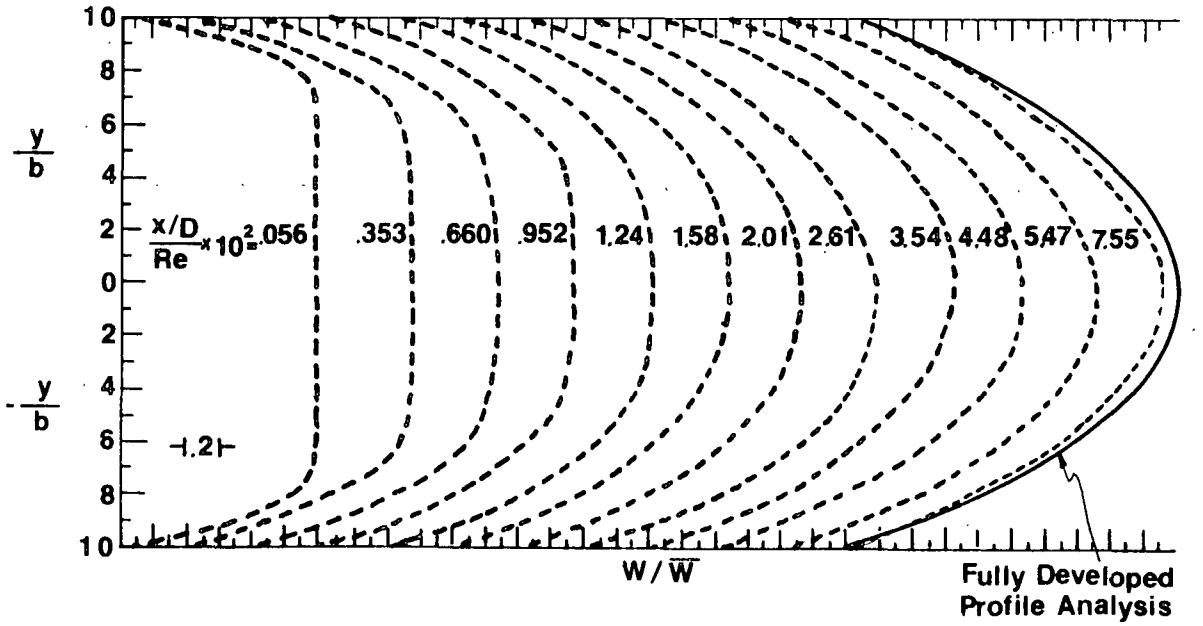

Figure 16. Velocity Development in Duct of 2:1 Aspect Ratio, Profiles Across Narrow Duct Dimensions (10)

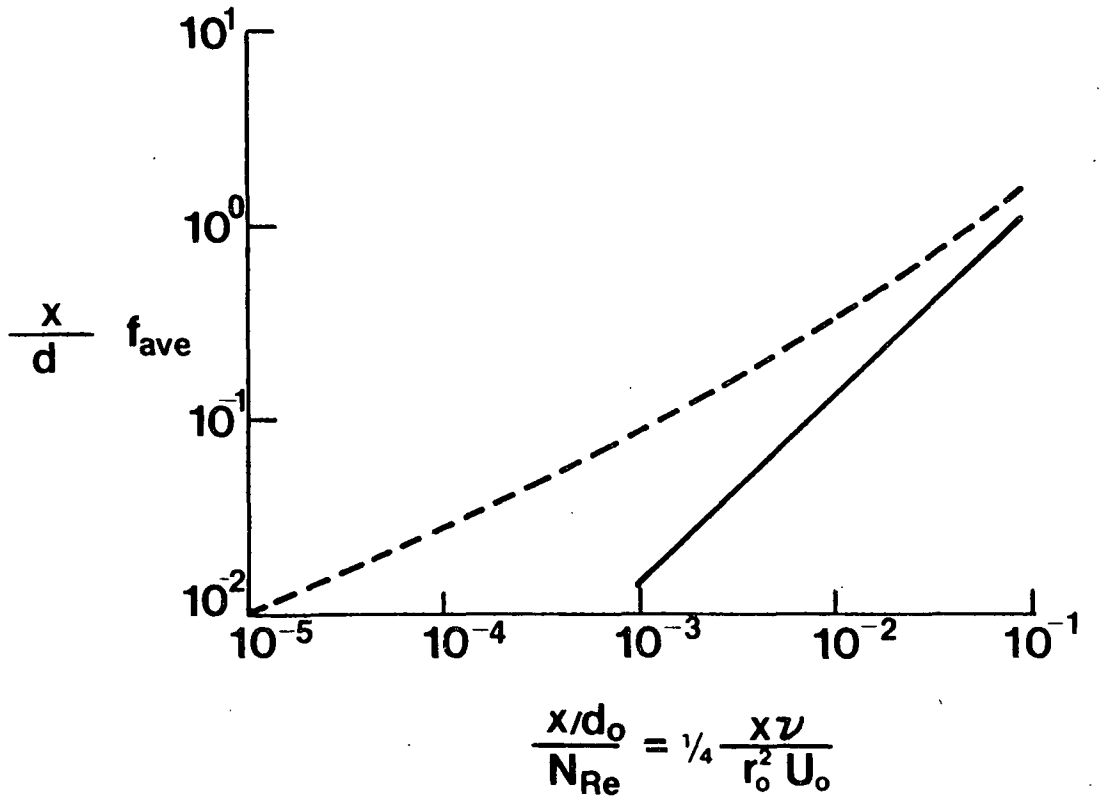

Figure 17. Average Friction Factor for the Entry Section of Pipe Flow (11)

CONSISTENCY IN THE REFINER

Since the measured input consistency was 0.1%, we were led to expect that a collection of stock in the tackle occurs. The fluid mechanics of the rotor/stator system apparently hold fiber in the system until an equilibrium condition exists. This characteristic would prevail nearly independently of input consistency until the input consistency would be raised to such a high level that the transport characteristic of the refiner that prevails at conditions of present commercial practice no longer apply. This is expected to occur at consistencies much greater than 4%.

$$C_{in} >> 4\%$$

There is a preponderance of qualitative data in the films to support this phenomenon. Tests have also been conducted measuring the functional relationship between refiner consistency and other system parameters (Fig. 18).

$$C_R = f\ (C_{in},\ \text{properties of the flow, geometrical characteristics})$$

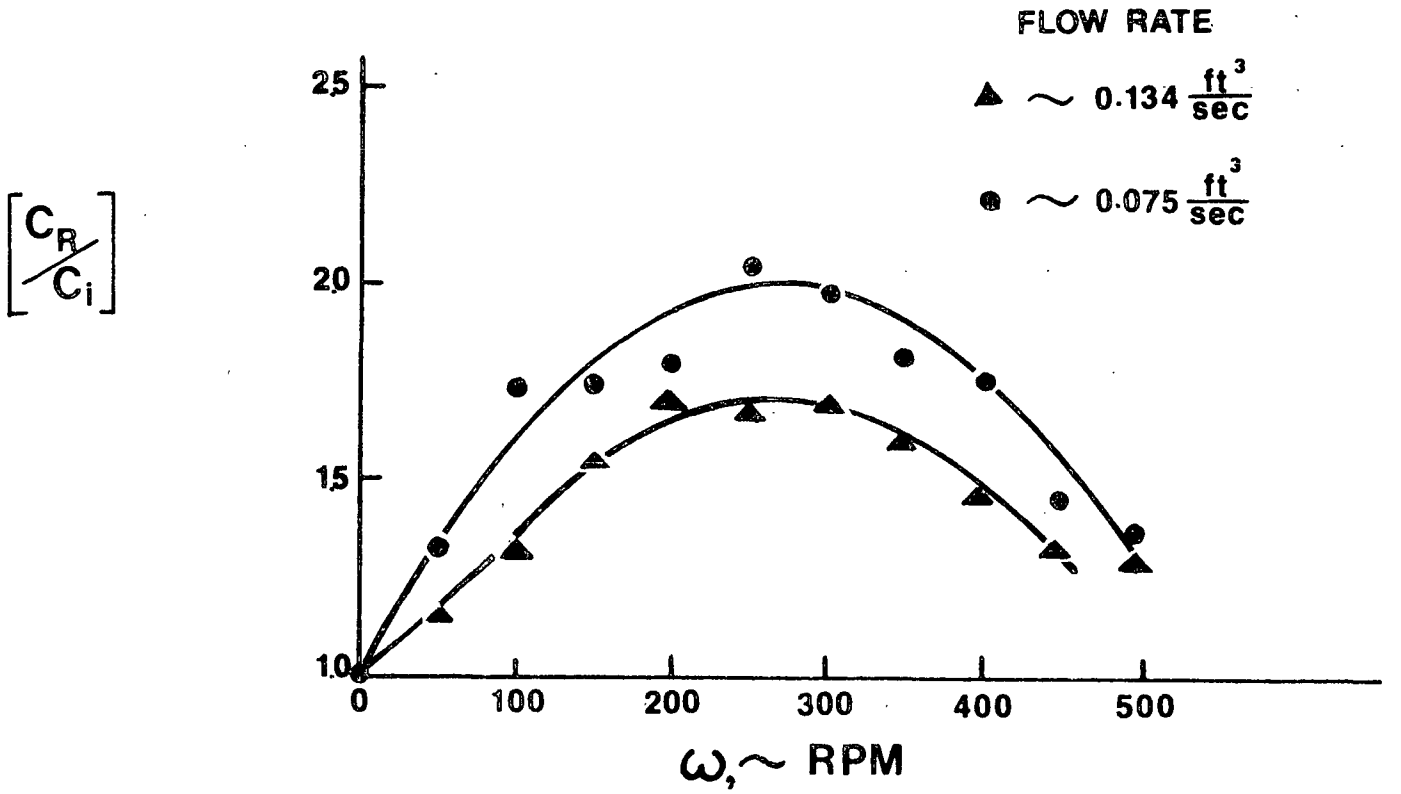

Figure 18. Typical Consistency Buildup in the Refiner

SECONDARY AND TERTIARY FLOWS

RECIRCULATION REGION

It can be expected from physical reasoning that primary, secondary, and tertiary flows will be present in the circulation region of the disk refiner. An outward radial flow in the rotor and an inward flow in the stator are to be expected in the circulation region. A small circumferential flow is also expected because of the rotational motion of the rotor. These three flows are arbitrarily called primary flows because they result from rather simplistic physical reasoning, and they have been confirmed by the visual studies.

If a cross section of a groove in the stator and the bar in the rotor is considered, then by virtue of the rotor bar motion with respect to the fluid in the stator groove, a rotational force is imposed on the fluid in the stator. This force sets up a vortex flow in the stator. The fluid in the groove of the rotor is forced into a similar vortex motion as the bars of the stator move with respect to the fluid in the groove of the rotor (Fig. 19).

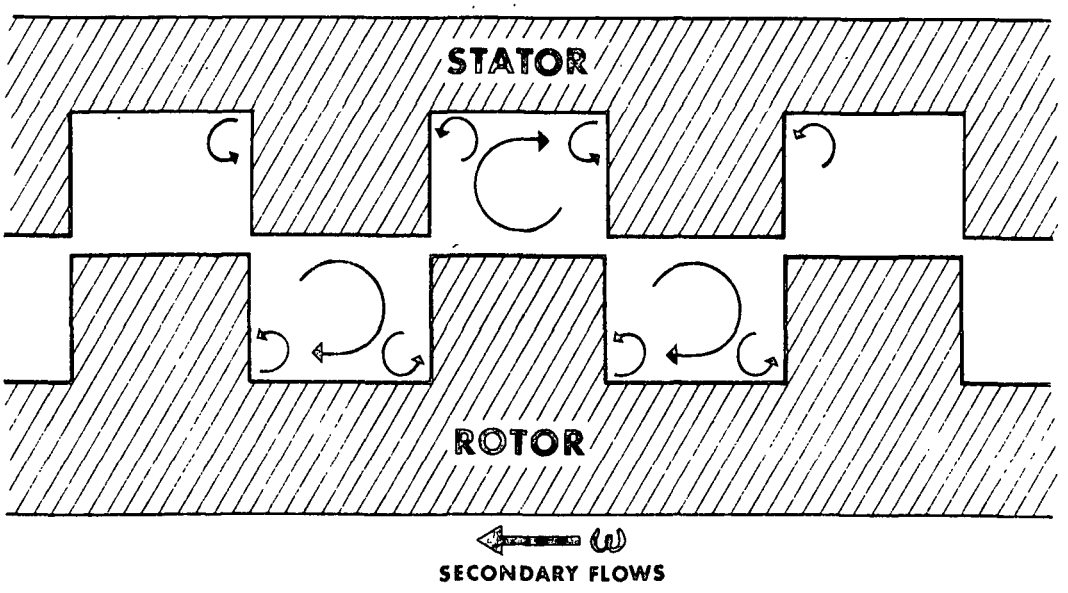

Figure 19

Note that these vortex flows are of the same rotational sense. Putting these secondary vortex motions together with the primary flow, it is apparent that the flow spirals outwards in the rotor and spirals inwards in the groove of the stator. In addition there might be secondary vortex flows in the corner regions.

Consider again a simplified flow model of one groove of the rotor and one groove of the stator; the flow in the rotor is greater than the flow in the stator [Equation (1) and Fig. 5]. Thus the velocity in the rotor is faster than the velocity in the stator and gives rise to the pressure in the stator being higher than the pressure in the rotor. Thus a pressure gradient exists in the direction across the cross section from the stator to the rotor. The magnitude of this pressure difference can be estimated from a simple Bernoulli balance. Then

$$\Delta p = \Delta\bar{u}^2/2 = 12.1 \text{ lb}_f/\text{ft}^2 \qquad (31)$$

for a typical test run on the refiner. Although this is a small pressure difference, it is very important as far as the refining mechanism is concerned and is the driving force behind the tertiary motion.

As previously indicated, a small secondary vortex could exist in the corner of the stator, but this does not occur because of the pressure gradient that exists from stator to rotor. In fact, the flow comes all the way down the leading edge of the stator bar as shown in Fig. 20 by the dashed line. This flow would be the source of the primary flow $\underline{Q}_C$ in the circumferential direction. This $\underline{Q}_C$ would further reduce the strength of $\underline{Q}_S$ and further strengthen the transverse pressure gradient. This tertiary flow is of importance since it prevents fiber from stapling over much of the stator and is distinguished from the secondary motions because it is a result of the small pressure gradient between the stator and rotor.

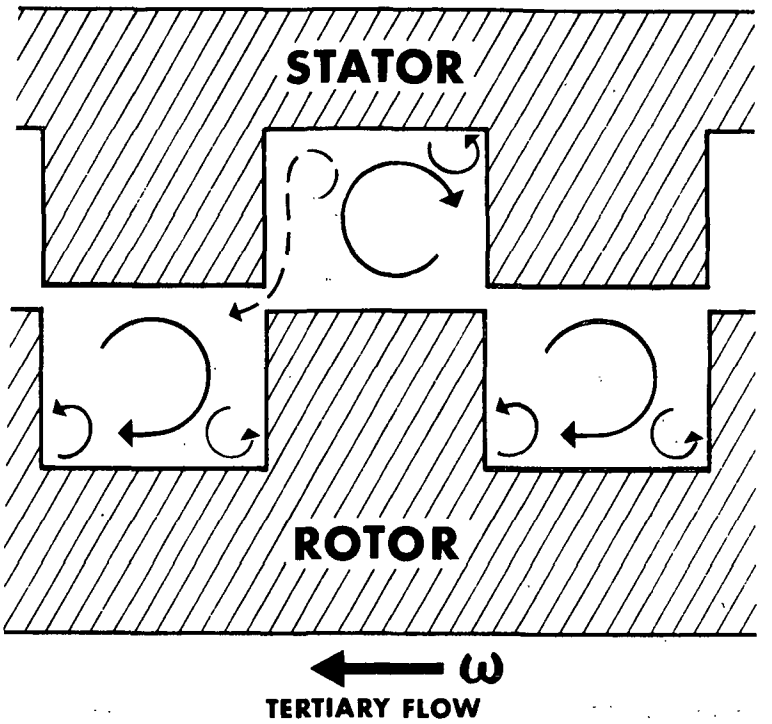

Figure 20

Putting all of these complex motions together, there is: a primary circumferential motion; a primary radial flow outward with a secondary vortex flow outward in the groove of the rotor; and a primary flow inward in the groove of the stator with a secondary vortex flow of the same angular sense as that of the rotor. Secondary motions exist in the corner of the grooves of both the rotor and stator with that in the stator modified to be a tertiary wiping flow at the leading edge. The wiping flow comes down and out of the stator and holds the pulp fibers against the bars of the rotor so that refining work can be done.

The visual observations show that the fibers lie across the leading edge of the rotor. The heads of the fibers are held down by the secondary vortex flow in the groove of the rotor. One might expect the same thing to occur on the leading edge of the stator bars, but this was not observed in the films except at the stator periphery. This does not happen because of the tertiary motion (Fig. 21).

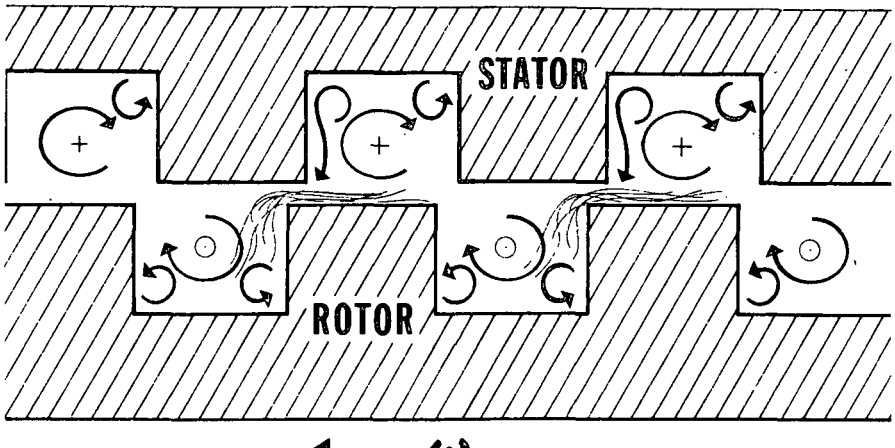

STAPLING OF FIBERS ON ROTOR

Figure 21

The fibers are stapled to the rotor or the stator, but not both the rotor and the stator at any particular radius. It is the conclusion of this work that this is where the refining takes place. The fibers align themselves principally along the rotor bar in a circumferential direction. Periodically, they may break loose and become a part of the inward stator flow (and may become stapled again), become part of the outward rotor flow and recycle to the stator flow at the periphery as was visually observed to often happen, or become part of the flow that eventually leaves the refiner through the outlet.

DISCHARGE OF REFINED STOCK

The functions of transport are at least stock input, circulation and delivery. Input seems to be a most simple process as a slurry of fiber and water is supplied by pipe under pressure. The circulation of stock is much more complicated. After circulation (and refining) the flow is then reunited and discharged to the outflow after the refining action is completed. It is apparent that refining, by definition, can only be accomplished during the circulation phase with some interactions between the fiber release and circulation likely. Clues to the mechanisms of discharge of beaten stuff from the disk refiner are apparent from the high-speed films. Some broad statements on the action of the

disk refiner can be made without serious risk of error. Several mechanisms for collection and discharge of refined fibers appeal to reason. Some may be rejected straightaway, while others can be tested experimentally to establish or preclude their credibility.

RELEASE DELIVERY

This mechanism behaves as follows. Fiber is in fact stapled to the leading edge of the rotor bars as observed in the films (Fig. 3). High fluid (and mechanical) shear acts to cut and refine the stock. These actions exert a force on the stapled fibers in a direction opposite to the direction of rotation of the rotor. Fiber is physically moved in the direction opposite to rotation as a result, and swept away by the circulating flow to be restapled and further refined, or if it is not restapled, it is delivered into the stock discharge.

SLIP DELIVERY

The fibers are (as before) stapled to the leading edge of the rotor tackle. The outward motion of the flow in the grooves of the rotor tackle imparts a radially outward drag force on the heads of the fiber. This force will drag stapled fiber off the bars and be delivered to the tackle periphery. It is known that fiber reaching the discharge periphery is not necessarily discharged from the refiner. A portion of the stock is recirculated back through the stator groove and is subject to restapling and repeated refining and destapling.

SWEEP DELIVERY

Note that on a line from the inflow source to the outflow sink, the so-called exit zone, conditions for delivery are most favorable. The imposed line pressure has its maximum gradient along this plane. In addition, the outward flow in the rotor does not stagnate in this region. A favorable pressure gradient, therefore, exists from the source to the sink in both the stator and the rotor tackle. This is the only zone in the refiner where this condition exists. As a result of these unique circumstances, a radially outward flow of stock in both the rotor and stator is established. This flow is also of higher velocity than at any other region in the refiner. This high velocity flow sweep delivers all the fibers off the tackle and delivers the flow to the periphery in close proximity to the discharge port of the refiner outflow (sink).

These three mechanisms for destapling have been observed with high-speed photography. Release delivery is not the only primary mode of delivery. A typical disk refiner has a circumference of about 100 inches and a typical land and groove characteristic dimension of approximately 0.3 inch. Therefore, there exists approximately 300 impacts/revolution and about 10 revolutions per second at 600 rpm.

Experimental observations of this mechanism show a time duration of no less than several seconds between release. Since restapling is likely, the order of impacts a fiber will receive is

$$I \mathcal{O} 10^4 \qquad (32)$$

Previous authors have held that the number of impacts experienced by fiber in the disk refiner is on the order of hundreds, not on the order of thousands. Thus, if release delivery is a major delivery mechanism important to the mechanics of refining, then previous authors have been in error.

It should be noted that slip delivery and sweep delivery are very similar and may reasonably be thought of as the same mode of delivery. The distinguishing difference between sweep and slip delivery is that slip delivery is a steady process with respect to the entire plane of the rotor/stator pair. During sweep delivery, slip occurs only in the region of the rotor/stator pair close to the line between the source and sink. Sweep delivery has been verified to be a primary delivery mode in the experimental refiner used in this work.

FLOW REGIONS

One is led to reason that there must exist an ω low enough that no refining takes place by virtue of insufficient secondary motion required to cause stapling (see Fig. 22). Let us assume that there is an ω_{st} (onset of stapling) sufficient to allow stapling but insufficient to cause sweep delivery. Under these conditions release delivery would dominate and a great deal of refining would necessarily result. An increase in ω to ω_{sw} (onset of sweep) would generate a strong enough flow to sweep delivery fiber to the discharge sink, a controllable situation. If ω were further increased to $\omega_{s\ell}$ (onset of slip), slip delivery would result. Finally, at ω_c (onset of cavitation), cavitation would result in a sharp decrease in refining action.

Experimental verification of the picture presented in Fig. 22 has been accomplished by use of the high-speed films and more simply with the aid of a stroboscope. The quantitative results of this work are presented in Fig. 23.

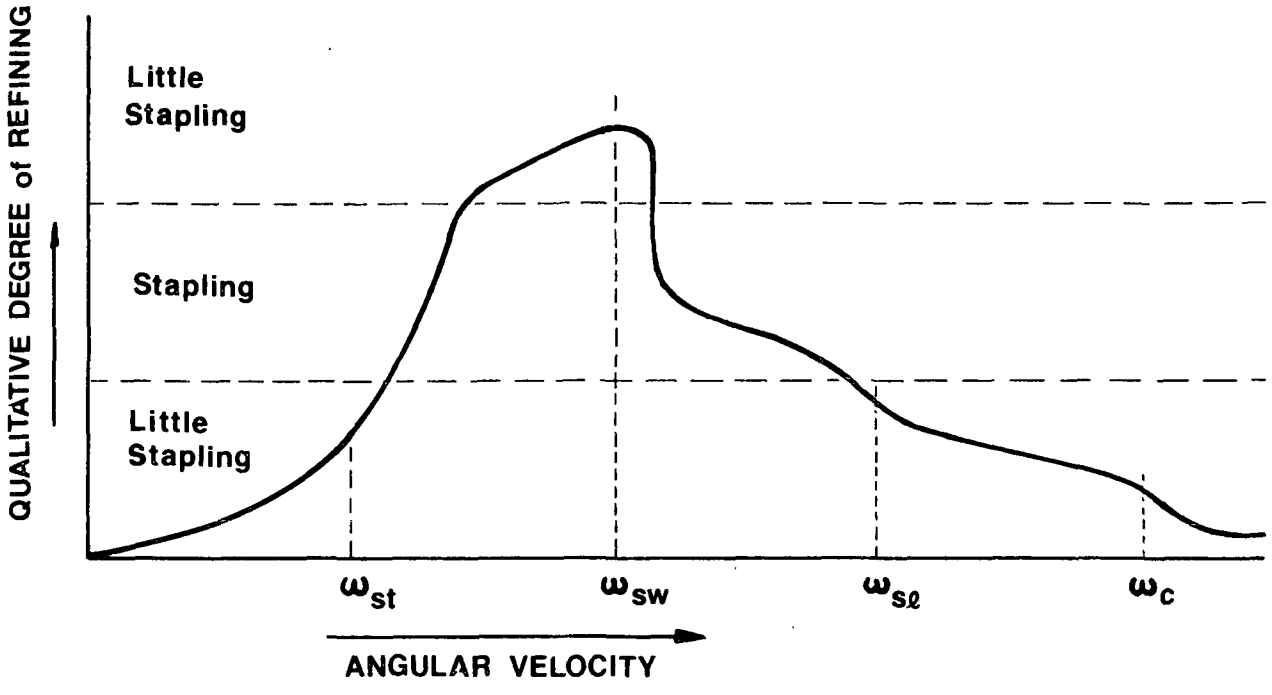

Figure 22. Qualitative Estimate of Expected Flow Regimes

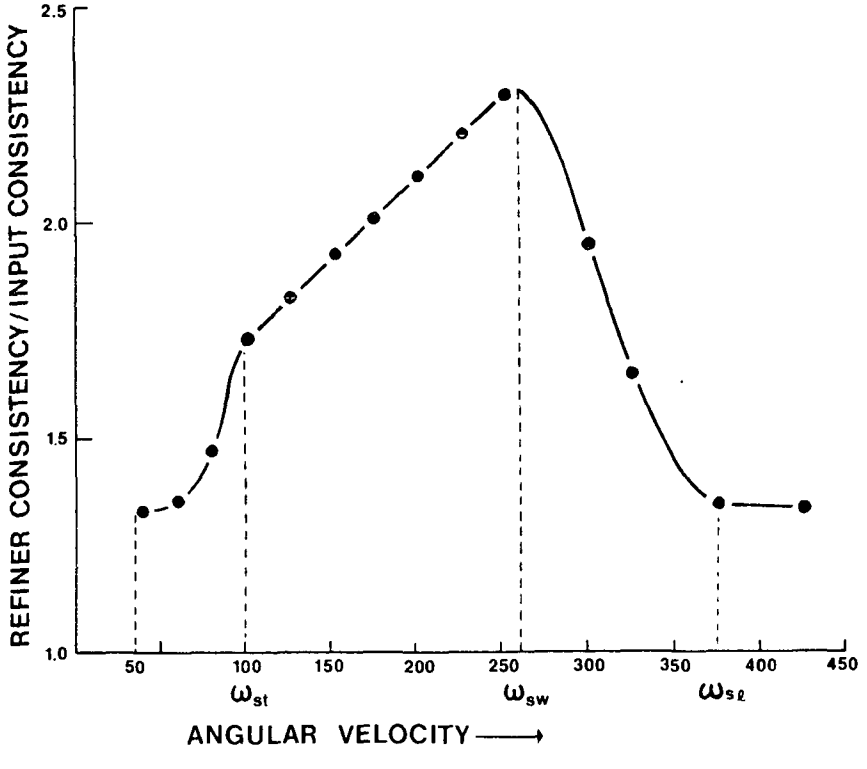

Figure 23. Flow Regimes Within the Refiner

Let us consider the operation of a disk refiner in the zone

$$\omega_{sw} < \omega < \omega_{s\ell} \tag{33}$$

Also let us assume that release delivery is not an important release mechanism. Then let us attempt to develop an understanding of the nature of the interactions between circulation, stapling, and refining.

RESIDENCE TIME

The average residence time that the fibers are retained within the refiner is important in the development of the relationship which expresses the frequency function of impacts received by individual fibers. There are several ways in which the residence time can be determined. An estimate can be made from the overall flows and a knowledge of the accumulation of fiber in the refiner. An alternate estimate can be made from the model of the refiner as proposed herein.

The overall estimate of the residence time can be made from

$$\tau = (L/\bar{u})\ (C_R/C_0) \tag{34}$$

where $\underline{L}$ is the path length for one pass of the flows and the ratio (C_R/C_0) accounts for the accumulation of fiber in the refiner. Figure 24 defines the path length, thus $\underline{L}$ is given by

$$L = \frac{\overline{abcd} + \overline{ad}}{2} = \frac{d}{4}\ (2 + \pi) \tag{35}$$

The velocity $\underline{\bar{u}}$ is simply

$$\bar{u} = Q_i/A \tag{36}$$

thus

$$\tau = \frac{d\ (2 + \pi)}{4\ (Q_i/A)}\ \ (C_R/C_0) \tag{37}$$

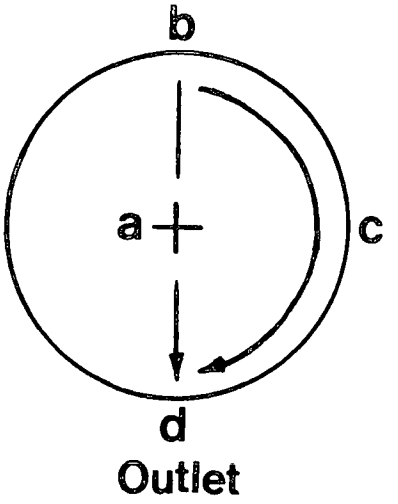

Figure 24. Determination of Average Path Length

For the experimental refiner (1 ft diameter) at an ω = 150 rpm, the ratio ($\underline{C}_R/\underline{C}_O$) is 1.54 for the flow of 60 gal/min (0.134 ft^3/sec). The appropriate cross sectional area is 0.09 ft^3 as previously given in Equation (15). Thus

$$\tau = \frac{1.28}{(0.134/0.09)} (1.54) \simeq 1.3 \text{ sec} \qquad (38)$$

An alternate estimation can be made based on the model of the flow. For an ω of 150 rpm, the time for one revolution is 0.4 sec. For the experimental refiner (1 ft diameter), the peripheral velocity would be the outer circumference divided by the time or 7.9 ft/sec. The approximate velocity in the grooves is 5 ft/sec [see Equation (19)]. Since the grooves are about 1/4 ft long, the time needed to sweep all the fiber out of the grooves would be 0.05 sec. Since the rotor makes one revolution in 0.4 second, one would need 12.5% of one revolution to sweep the grooves clean. This corresponds to 45°. However, the exit is 1 inch, which corresponds to 9-1/2° of the periphery. Thus, 21.1% of the fiber can be removed per revolution or equivalently each fiber on the average experiences 4.7 revolutions. Since each revolution requires 0.4 second, the residence time is

1.9 seconds. This compares favorably with the overall estimate of 1.3 seconds. An average estimate would be 1.6 seconds.

In the circulation region it can be calculated that the time to sweep a groove clean is 0.05 second. The average number of times a fiber can loop in the circulation region can be estimated by dividing the residence time by the time for one loop, which gives 16 loops. This certainly would allow adequate contact to provide stapling.

NUMBER OF IMPACTS

It is assumed that effective refining only occurs when fibers are stapled to either the rotor or the stator. It has been observed that fibers are stapled predominantly to the bars of the rotor.

The impacts imparted to a stapled fiber are then

$$I = \Omega \tau N_s \left[1 - \frac{\theta_2 - \theta_1}{2\pi}\right] f(\theta) \qquad (39)$$

where

$\underline{I}$ = the average number of impacts

Ω = the revolutions per second

τ = the residence time

$\underline{N_s}$ = the number of stator bars

$\underline{f}(\theta)$ = the effective stapled fraction

The function $\underline{f}(\theta)$ is necessarily zero at $\theta = \theta_2$ and a maximum value at $\theta = \theta_1$. Throughout the recirculation region the high circulation out of the rotor and in the stator provides ample mixing and, therefore, opportunity for contained fibers to be stapled and refined. Qualitatively the stapled fraction must take the form shown in Fig. 25 when expressed as a function of θ.

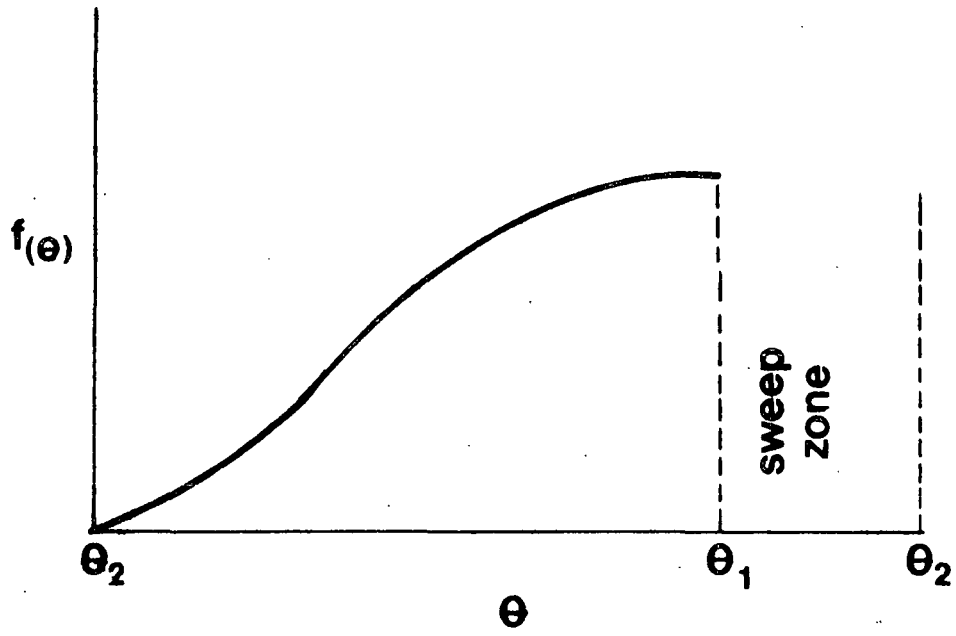

Figure 25. Fiber Stapling as a Function of Position Within the Refiner

The source of the fibers being stapled is the volume of stock contained in the tackle and the periphery between the tackle and the housing. The input stock consistency is, of course, equal to the output stock consistency and, therefore, is ignored. The qualitative value of the function $\underline{f}(\theta)$ is easily determined experimentally. Recognize that in a single revolution of the rotor, of all the fibers contained, a number ($\underset{\sim}{f}_{\underline{st}}$) will be stapled and will depend on θ. By drawing a test quantity of stock out of the periphery in close proximity of the rotor grooves, the number of fibers stapled is measured (Fig. 26). Then

$$\overline{f(\theta)} = \int \frac{f(\theta)\, d\theta}{n d\theta} \tag{40}$$

A graphical integration from Fig. 26 gives $\overline{\underline{f}(\theta)} \underline{\simeq} 0.35$ which seems reasonable. For the same conditions, the estimate for the number of impacts from Equation (36) is

$$I = \Omega\, \tau\, N_s \left(1 - \frac{\Delta\theta}{2\pi}\right) f(\theta) \tag{41}$$

$$= 2.5\ (1.6)\ 90\ (5/6)\ (0.35) \underline{\simeq} 100 \text{ impacts}$$

for the experimental refiner. For a commercial refiner, the number of impacts may well be in excess of 10^3 as is seen from Equation (41).

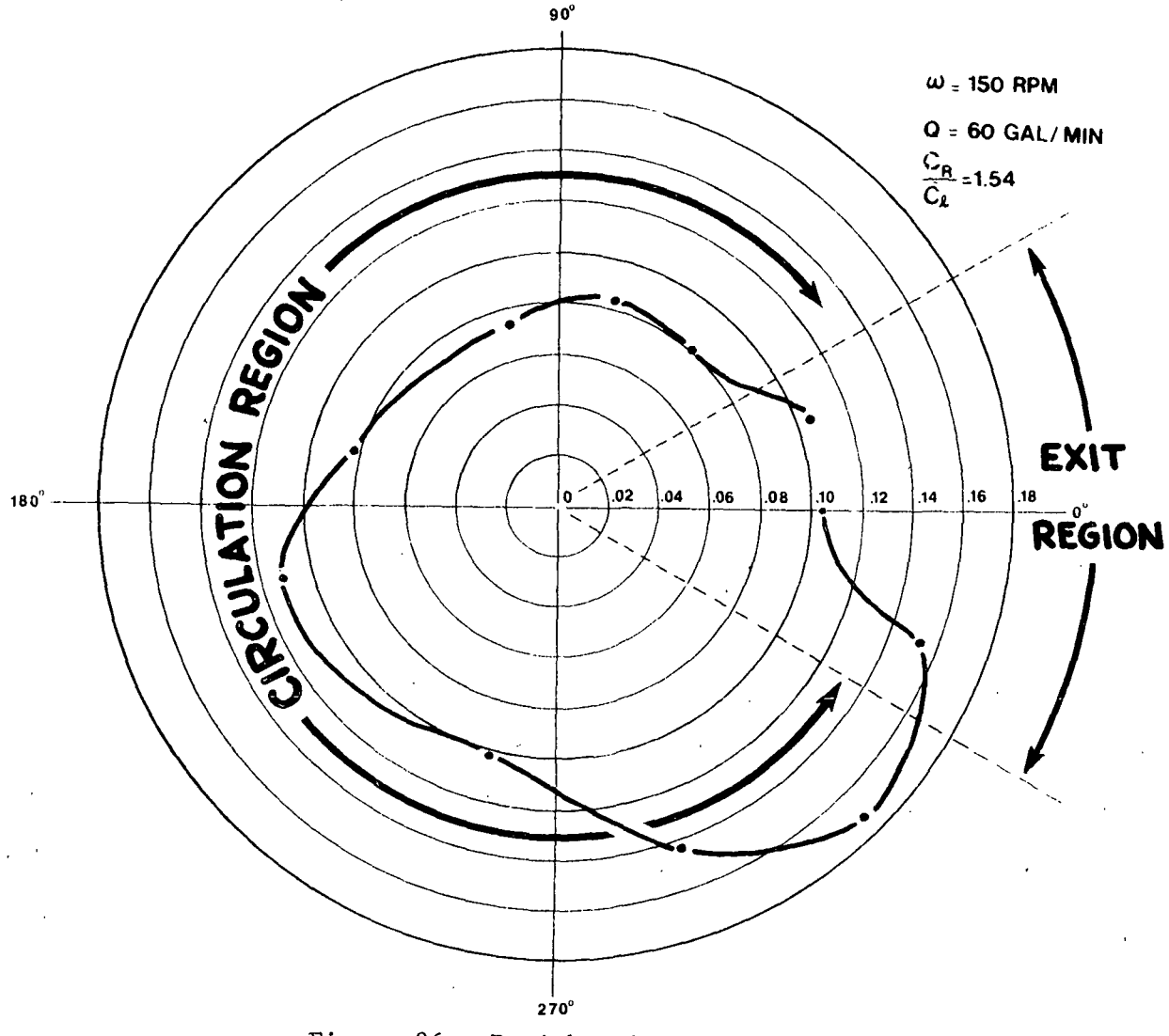

Figure 26. Peripheral Consistency

CONCLUSIONS

The present work used, as a basis, the approach of modern high-speed photography to attempt to establish the fluid mechanics and related transport mechanisms involved in a disk refiner. The clear Plexiglas construction of the refiner, the mixtures of dyed and undyed fibers, and a modern photographic system easily capable of framing rates in excess of 10,000 per second made the study possible.

Based on the visual observations, a reasonable transport mechanism and model for the fluid and fiber motions was made and additional measurements of the pressure field provided for its verification. Within the refiner there is considerable build-up of consistency. The fibers are primarily stapled to the rotor and move in a flow that is a complicated three-dimensional field involving primary, secondary and tertiary flows. It would appear that the refining action occurs to the fibers while they are stapled to the rotor and alternately pass the stator lands. The release of the fiber stock to the exit stream primarily occurs in an exit region by a mode called sweep delivery. The model of the flow field accounts for all the complex flows observed and allows estimation of fiber retention time and a number of rotations a fiber stays in the refiner as an average. Clearly, such estimates can lead to upper bounds for the number of impacts experienced by a fiber and this, in turn, is a first important step for relating the fluid fiber transport to refining.

NOMENCLATURE

Symbols that were not clarified in the text are listed below.

$\underline{A}$	average, rotor/stator cross-section area
$\underline{C_i}$	input consistency
$\underline{C_{in}}$	inlet consistency
$\underline{d}$	diameter
$\underline{d_e}$	equivalent diameter
$\underline{f}(\theta)$	effective stapled fraction
$\underline{f_{st}}$	number of stapled fibers
$\underline{I}$	number of impacts
$\underline{\ell}$	tackle length
$\underline{m}$	source or sink strength
μ	absolute viscosity
ν	kinematic viscosity
$\underline{N_E}$	entry length number
$\underline{N_s}, \underline{N_r}$	number of stator/rotor grooves or lands
$\underline{N_{Re}}$, Re	Reynolds number
$\sim$	on the order of
ω	angular velocity
ω_c	angular velocity at onset of cavitation
$\omega_{s\ell}$	angular velocity at onset of slip
ω_{st}	angular velocity at onset of stapling
ω_{sw}	angular velocity at onset of sweep
$\underline{P_d}$	stagnation pressure
$\underline{P_{drag}}$	pressure friction losses
$\underline{P_\ell}$	imposed status pressure field

Q	volume flow rate
Q_C	circumferential volume flow rate
Q_I	input volume flow rate
Q_O	output volume flow rate
Q_P	peripheral flow
Q_R	rotor volume flow rate
Q_S	stator volume flow rate
ρ	density
r,θ	polar coordinates
r_e	equivalent radius
r_H	hydraulic radius
r_o, r_i	outer and inner radius of the tackle
t	time or characteristic tackle dimension
τ	shear stress, residence time
u,v	velocity components
$\bar{u},\bar{v}$	average velocity components
U_I	input velocity
$\bar{u}_{s,r}$	average velocity in the stator/rotor
x,y,z	rectangular coordinates
z	complex plane

LITERATURE CITED

1. Banks, W. A., Paper Technol. 8(4):367(1967).

2. Atack, D., and May, W. D. High speed photography of particle motion in a disk refiner. Proc. 9th Intern. Congress, High Speed Photography Soc., Motion Picture and Television Engineer, New York. 2nd Printing, 1970.

3. Brodkey, R. S. Stereoscopic flow visualization. Proc. Intern. Conf. on Flow Visualization, Tokyo, October, 1977.

4. Schlichting, H. Boundary layer theory. 4th ed. New York, McGraw-Hill, Inc., 1960.

5. Langhaar, H. L. Steady flow in the transition length of a straight tube. J. Appl. Mech. 9, Trans. ASEM 65:55-8(1942).

6. Brodkey, R. S. Phenomena of fluid motions. Reading, MA, Addison-Wesley Publishing Company, 1967.

7. White, F. M. Viscous fluid flow. New York, McGraw-Hill, Inc., 1974.

8. Guthrie, W. E. An apparent viscosity for use in the application of Reynolds numbers to the flow of dilute pulp suspensions. Tappi 42:3(1959).

9. Metzner, A. B., and Reed, J. C. Flow of non-Newtonian fluids — Correlations of the laminar, transition, and turbulent-flow regions. AIChE J. 1(4):434-40 (1955).

10. Sparrow, E. M., Hixon, C. W., and Shavit, G. Experiments on laminar flow development in rectangular ducts. J. Basic Eng., Trans. ASME, Series D, 89:116-24(1967).

11. Knudsen, J. G., and Katz, D. L. Fluid dynamics and heat transfer. New York, McGraw-Hill, Inc., 1958.

THE INSTITUTE OF PAPER CHEMISTRY

Terrence S. Fox
Director
Engineering Division